

# Shear Wave Velocity Profiling by the SASW Method at Selected Strong-Motion Stations in Turkey

B. Rosenblad<sup>1</sup>, E.M. Rathje<sup>2</sup> and K.H. Stokoe, II<sup>2</sup>

<sup>1</sup> Research Associate, University of Texas at Austin, ECJ 9.227

<sup>2</sup> Assistant Professor and Jennie C. and Milton T. Graves Professor, respectively, University of Texas at Austin, ECJ 9.227

## Abstract

The 1999 Izmit and Duzce earthquakes in Turkey have generated important information and data at stations where strong ground motions were recorded and sites where significant soil liquefaction occurred. One key variable in investigating the earthquake response at these sites is the shear stiffness profile of the subsurface soils. Researchers at the University of Texas at Austin (UT) conducted a joint study with Utah State University (USU) to characterize small-strain shear wave velocity profiles at selected sites using in situ seismic measurements. UT personnel were responsible for determining shear wave velocity profiles at 20 strong motion stations. These evaluations were performed using the spectral-analysis-of-surface-waves (SASW) method and extended to depths between 6 and 45 m, depending on spatial and source considerations. The velocity profiles and associated information are presented in this report. Profiling at liquefaction sites was performed by USU personnel and these results are presented in a companion report (reference to be added).

## Introduction

The 1999 Izmit ( $M_w = 7.4$ ) and Duzce ( $M_w = 7.1$ ) earthquakes in Turkey have generated enormous interest and excitement in the earthquake engineering community for several important reasons. First, a large number of strong motion stations successfully recorded these earthquakes and their aftershocks (Figure 1). Second, prior to these events, there were less than ten ground motion recordings for  $M_w \geq 7.0$  earthquakes at distances less than 20 km from the fault rupture. Six recordings were made during the Izmit earthquake within 20 km of the fault rupture and six recordings were made during the Duzce earthquake within 20 km of the fault rupture. Third, the Izmit earthquake induced severe liquefaction in many areas. The most extensive liquefaction was observed in the city of Adapazari, approximately 7 km north of the fault rupture (Figure 1). Liquefaction-induced settlement, tilting, and bearing capacity failures were documented (EERI 2000). Characterization of these soils will permit a more complete assessment of our current liquefaction evaluation procedures, expand our database of liquefaction case histories, and understand more fully the interaction between site effects and liquefaction response within alluvial basins.

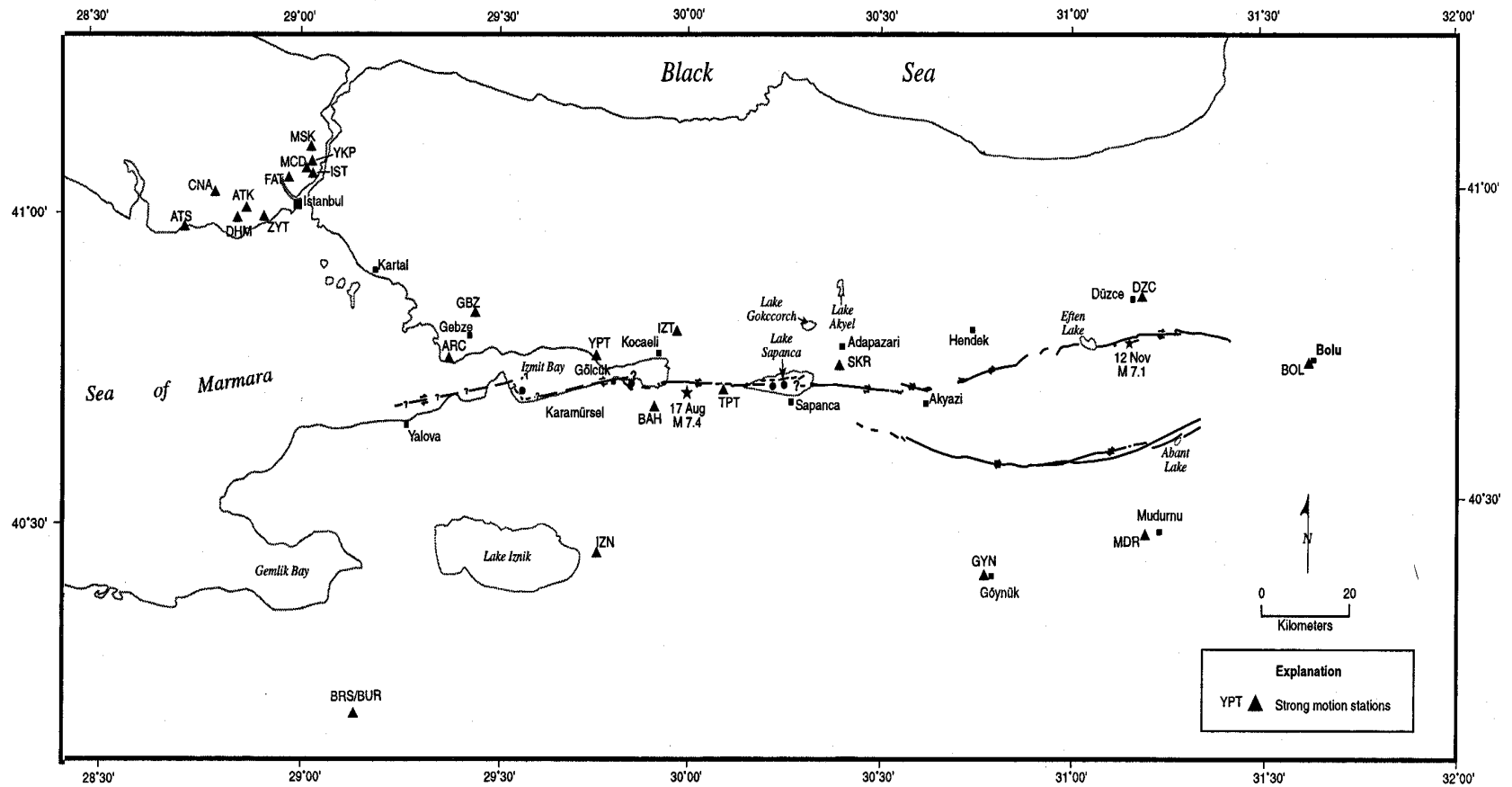


Fig. 1 Location of Strong Motion Stations with Respect to the 1999 Kocaeli and Duzce Earthquakes (courtesy of William Lettis and Associates, Walnut Creek, CA)

The main goal of the study presented in this report was to characterize the small-strain shear modulus at key geotechnical sites shaken during the 1999 earthquakes in Turkey. In situ characterization of the small-strain shear moduli was done using seismic measurements of shear wave velocities. To perform the in situ seismic measurements, a nonintrusive seismic testing technique involving Rayleigh-type surface waves was used. This technique is called the spectral-analysis-of-surface-waves (SASW) (Stokoe et. al., 1994). The technique is nonintrusive because both the source and receivers are placed on the ground surface. Measurement of surface wave dispersion is performed in the field, and forward modeling is used in the laboratory to evaluate the shear wave velocity profile at the site. Shear wave velocity profiles from 16 strong-motion stations and 4 aftershock stations are presented here. These profiles extend to depths between 6 and 45 m.

This research study is a joint study between Drs. K. Stokoe, II and E. Rathje at the University of Texas at Austin (UT) and Dr. J. Bay at Utah State University (USU). UT researchers focused on evaluating strong-motion stations, while USU researchers tested mainly liquefaction sites. Only the results from testing at the strong-motion stations are presented here. Results from the liquefaction investigations are presented in a companion report (reference to be added).

### **Strong Motion and Aftershock Stations Tested**

Twenty strong-motion stations were tested as part of this study (Table 1). Testing focused mainly on near-fault stations, typically within 30 km from the fault. The near-fault stations tested from the Izmit earthquake are Sakarya (SKR, 3.3 km), Yarimca (YPT, 4.4 km), Izmit (IZT, 5 km), Duzce (DZC, 12.5 km), Gebze (GBZ, 13.5 km), Arcelik (ARC, 21.6 km), and Iznik (IZN, 29.7 km). Two sites in western Istanbul (Ambarli [ATS, 78.9 km] and Cekmece [CNA, 76.1 km]) were also tested because of the unusually large ground motions recorded at these strong-motion stations from the Izmit earthquake (EERI 2000). The near-fault stations tested from the Duzce earthquake are Bolu (BOL, 17.6 km) and 6 temporary recording stations installed by the Lamont-Dougherty (LD) Observatory of Columbia University. The LD stations tested are LD-7 (1 km), LD-5 (11.4 km), LD-12 (13.3 km), LD-10 (15.6 km), LD-3 (27.4 km), and LD-9 (30.2 km). These stations are all located west of the Duzce earthquake fault rupture. Additionally, two aftershock stations in the Duzce alluvial valley (Ballica and Aydipinar) and two aftershock stations in Yalova (Hastane and Hilal), all installed by the Kandilli Observatory and Earthquake Research Institute, were tested.

### **SASW Testing Method**

The basis of the SASW technique is the dispersive property of Rayleigh-type surface waves when propagating in a layered system. Dispersion refers to the variation of Rayleigh wave phase velocity with wavelength (or frequency). Dispersion arises because Rayleigh waves of different wavelengths sample different depths in a material profile as illustrated schematically in Figure 2. As wavelength increases, particle motion extends to greater depths in the profile. The velocities of Rayleigh waves, or surface waves, are representative of the material stiffness over depths where there is significant particle motion. For example, the particle motion of a wave that has a wavelength less than the thickness of the top layer is confined to this layer (Figure 2b).

Table 1. Strong Motion Stations And Aftershock Stations Tested As Part Of This Study.

| Station (Owner <sup>1</sup> ) | Records <sup>2</sup> | Distance <sup>3</sup><br>(km) |
|-------------------------------|----------------------|-------------------------------|
| Arcelik – ARC (K)             | IZT / DZC            | 21.6 / 135.7                  |
| Ambarli – ATS (K)             | IZT / DZC            | 78.9 / 193.3                  |
| Bolu – BOL (E)                | - / DZC              | - / 17.6                      |
| Cekmece – CNA (K)             | IZT / DZC            | 76.1 / 188.4                  |
| Duzce – DZC (E)               | IZT / DZC            | 12.5 / 8.2                    |
| Gebze – GBZ (E)               | IZT / -              | 13.5 / -                      |
| Izmit – IZN (E)               | IZT / -              | 29.7 / -                      |
| Izmit – IZT (E)               | IZT / -              | 5.0 / -                       |
| Sakarya – SKR (E)             | IZT / DZC            | 3.3 / 49.9                    |
| Yarimca – YPT (K)             | IZT / DZC            | 4.4 / 101.7                   |
| LD-3 (L)                      | - / DZC              | - / 27.4                      |
| LD-5 (L)                      | - / DZC              | - / 11.4                      |
| LD-7 (L)                      | - / DZC              | - / 0.9                       |
| LD-9 (L)                      | - / DZC              | - / 30.2                      |
| LD-10 (L)                     | - / DZC              | - / 15.6                      |
| LD-12 (L)                     | - / DZC              | - / 13.3                      |
| Ballica – BAL (K)             | - <sup>4</sup>       | -                             |
| Aydinpinar – AYD (K)          | - <sup>4</sup>       | -                             |
| Hastane – HAS (K)             | - <sup>4</sup>       | -                             |
| Hilal – HIL (K)               | - <sup>4</sup>       | -                             |

<sup>1</sup> Owners: E – Earthquake Research Department  
K – Kandilli Observatory  
L – Lamont Doherty Observatory

<sup>2</sup> Events recorded at each station  
(IZT – Izmit earthquake, DZC – Duzce earthquake).

<sup>3</sup> Closest distance to fault for each event

<sup>4</sup> Aftershock station

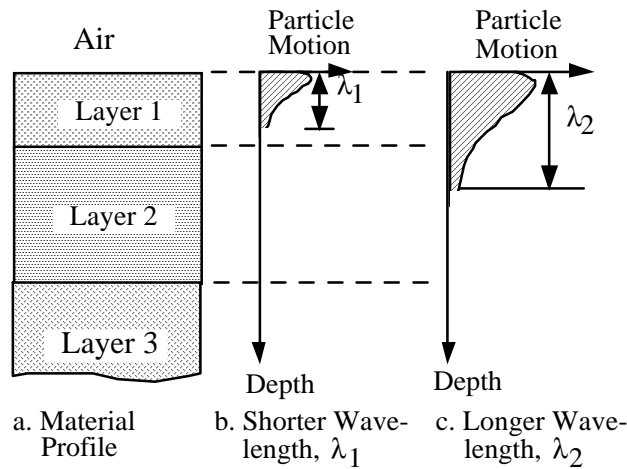


Figure 2 Approximate Distribution of Vertical Particle Motions with Depth of Two Surface Waves of Different Wavelengths (after Rix And Stokoe, 1989)

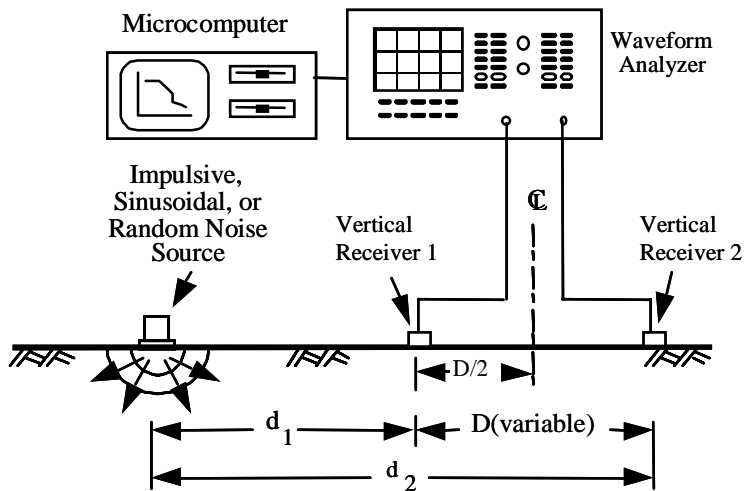


Figure 3 Traditional Configuration of Equipment Used in SASW Testing with a Two-Channel Recording System (Stokoe et al, 1994)

Therefore, the wave velocity is influenced only by the stiffness of the top layer. The velocity of a wave with a wavelength that is longer than the thickness of the top layer, but shorter than the combined thicknesses of the top two layers (Figure 2c), is influenced by the properties of only the upper two layers because essentially all motion occurs in these layers. Thus, by using surface waves with a range of wavelengths, it is possible to assess material properties over a range of depths.

SASW testing consists of making field measurements of surface wave phase velocity,  $V_R$ , at numerous wavelengths,  $\lambda_R$ , and using these measurements to calculate a dispersion curve for the site. A dispersion curve displays the variation in surface wave velocity with wavelength

(or frequency). The general field configuration of the source, receivers, and recording equipment typically used when testing with two receivers is shown in Figure 3. Surface waves are generated by applying a dynamic vertical load to the ground surface. Various mechanical and electromechanical sources have been used (Gucunski and Woods 1991, Stokoe et al. 1994, and Stokoe et al. 1999). At sites where there are no surface area limitations, the primary consideration in selecting a wave source is the required depth of profiling. Deep profiling requires a high-energy, low-frequency wave source, while shallow profiling can be done with a low-energy, high-frequency wave source. The propagation of these waves along the surface is monitored with the two receivers placed at distances of  $d_1$  and  $d_2$  from the source. Additionally, distance  $d_2$  is usually kept equal to two times  $d_1$ . Typical receiver spacings for deep profiling are 2, 4, 8, 16, 32 and 64 m. These spacings allow evaluation of most soil profiles to a depth of 50 to 70 m.

Different wave sources were used at different sites, depending on the receiver spacings, accessibility, and surface area constraints. Hammers and a 50-kg drop weight were used as wave sources at the shorter receiver spacings. For long receiver spacings (16 to 64 m) that were used to profile to larger depths, a large walking bulldozer was used as a low-frequency, high-energy wave source. The bulldozer operator continuously walked the bulldozer forwards and backwards, approximately 3 m in each direction, so that the distance between the source and receiver never became less than the spacing between the receivers. At stiff soil sites, walking bulldozers usually generate significant wave energy between 4 and 20 Hz, and usually produce maximum wavelengths of 100 to 200 m.

After the field data are recorded, a dispersion curve is calculated. For testing with multiple receivers, receiver pairs are used to determine the dispersion curve. For each receiver pair, the time histories recorded by the two receivers are transformed to the frequency domain, and the cross power spectrum and coherence function are calculated. It should be noted that all of these frequency domain quantities are calculated in real time by the waveform analyzer. The key data consist of the phase of the cross power spectrum and the coherence function. The coherence function represents a signal-to-noise ratio and is often close to one in the range of acceptable data. The time delay between receivers as a function of frequency,  $t(f)$ , is calculated from the phase of the cross power spectrum. The surface wave velocity,  $V_R$ , is calculated using:

$$V_R = (d_2 - d_1)/t(f) \quad (1)$$

The corresponding wavelength of the surface wave,  $\lambda_R$ , with a given frequency,  $f$ , is calculated by:

$$\lambda_R = V_R/f \quad (2)$$

The result of these calculations is a dispersion curve ( $V_R$  versus  $\lambda_R$ ) for each receiver pair. For the traditional two-channel SASW testing illustrated in Figure 3, individual dispersion curves from a group of receiver spacings are assembled together to form the composite dispersion curve for the site. An example of a composite dispersion curve is presented in Figure 4 using eight different receiver spacings as noted in the figure.

After a dispersion curve is calculated from the field data, forward modeling is used in the laboratory to evaluate the shear wave velocity profile. Forward modeling is the process of calculating the shear wave velocity profile by a trial-and-error matching of a theoretical dispersion curve with the measured field dispersion curve. In this process, the theoretical dispersion curve is calculated for an assumed velocity profile using the dynamic stiffness approach developed by Kausel and Roesset (1981). The computer program WinSASW (Joh 1996) is used for this purpose. The assumed velocity profile should contain a sufficiently large

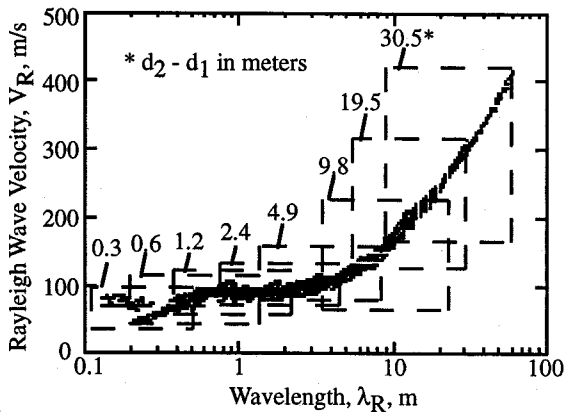


Figure 4 Composite Experimental Dispersion Curve from Traditional SASW Testing at a Soil Site (Stokoe et al. 1994).

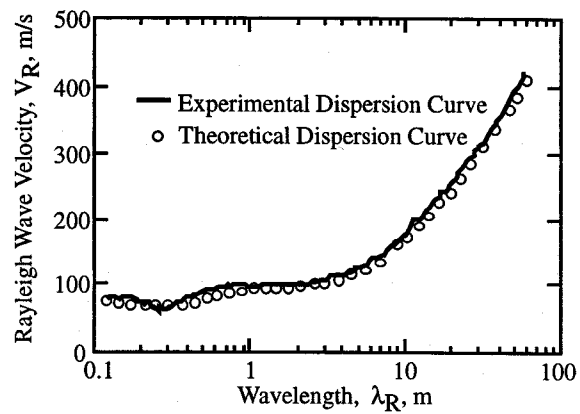


Figure 5 Comparison Between Experimental and Theoretical Dispersion Curves for a Soil Site (Stokoe et al. 1994).

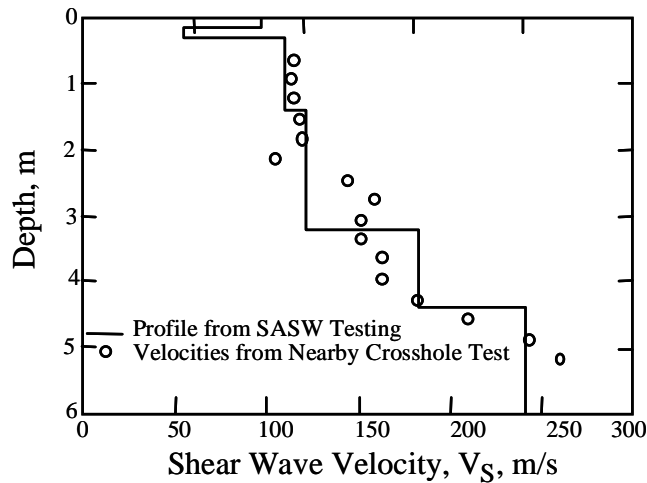


Figure 6 Shear Wave Velocity Profiles Determined from SASW (using the data shown in Figures 4 and 5) and Crosshole Tests at the Same Site (Stokoe et al. 1994).

number of sublayers to define the variation of material properties at the site. The shear wave velocities and thicknesses of the sublayers in the assumed profile are adjusted by trial and error until a satisfactory match between the theoretical and field dispersion curves is obtained. Such a match is illustrated in Figure 5 for the smoothed composite dispersion curve developed from the data shown in Figure 4. The resulting shear wave velocity profile is shown in Figure 6, along with results from crosshole tests also performed at this site (from Stokoe et al. 1994).

### **Example SASW Results from the Strong Motion and Aftershock Stations**

The results from SASW testing performed at the strong-motion and aftershock stations can be divided into three general categories. Results from three sites are presented below to demonstrate the characteristics of each category. First, results are presented from a site where deeper profiling was successfully performed and  $V_{S-30}$  was determined. The site is laterally uniform and analysis of the results is straightforward. Second, the results from a site that is not laterally uniform within the top 30 to 50 m are presented. These results also demonstrate one of the strengths of global measurements with the SASW method; that is, some indication of lateral uniformity over the tested area is determined. Finally, test results are presented from one remote site where surface access was limited and only smaller, hand-operated sources could be used to perform the tests. In this case,  $V_{S-30}$  could not be determined because the profile did not penetrate 30 m.

#### ***Example 1: Deep Profile and Laterally Uniform Site***

The results presented below were measured at the Ballica site discussed later in the report and noted in Table 1. At this location there was easy access for use of the bulldozer at the end of the SASW array, and a long stretch of flat unobstructed land existed through a field of poplar trees. Therefore, the SASW array was easily deployed over the desired distances and good quality data were recorded. Figure 7a shows the experimental dispersion curve measured at this location. The boxes in this figure indicate the portions of the dispersion curve measured with the six different receiver spacings used at this site. The dispersion curve covers a wavelength range of 0.6 m to 70 m which is sufficient to develop a shear wave velocity profile to a depth of 35 m. It is notable that over the entire range of the experimental dispersion curve there is very good consistency between portions of the dispersion curve measured with different receiver spacings. This consistent overlap indicates a laterally consistent profile over the extent of the SASW array. This attribute allowed a single theoretical dispersion curve to be fit to the experimental dispersion curve and a shear wave velocity profile to be determined to a depth of 35 m. The theoretical dispersion curve is presented in Figure 7b, and the resulting profile is presented in Figure 8 and Table 2. The columns in Table 2 labeled P-wave velocity and S-wave velocity represent the compression wave and shear wave velocities, respectively. Above the water table, the compression wave velocity was not measured but was assumed indirectly by assuming values of Poisson's ratio combined with the shear wave velocities. Below the water table the compression wave velocity of 1500 m/s was assumed and the resulting Poisson's ratio was calculated. Knowledge of the depth of the water table is important in these assumptions. The  $V_{S-30}$  value used for UBC classification was easily determined at this location.

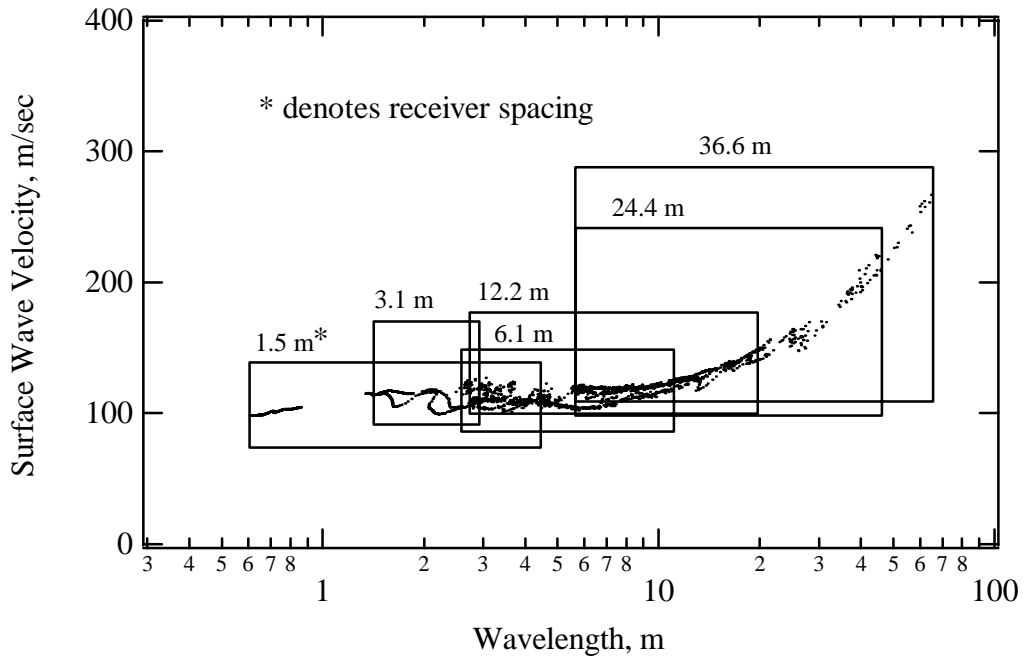


### ***Example 2: Deep Profile and Laterally Variable Site***

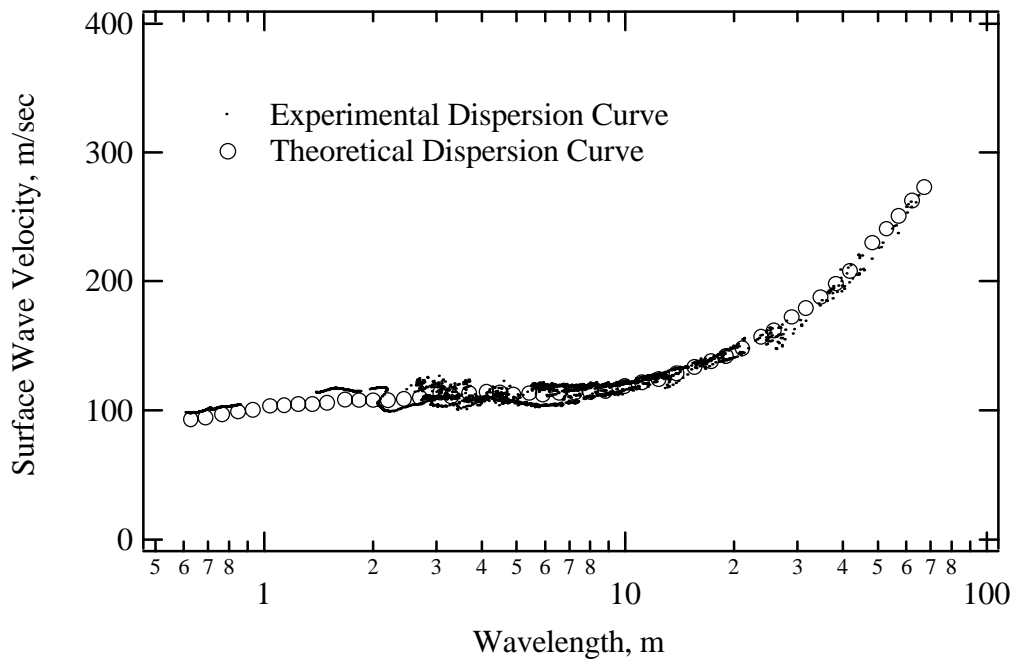
The results presented below were measured near the Arcelik station located on the Arcelik industrial facility north of Gebze. At this location there was sufficient access for use of the bulldozer source and a flat expanse of land for the deployment of the SASW array. The experimental dispersion curve measured at this site is presented in Figure 9a. The boxes in this figure show the contribution of each receiver spacing in the array to the total dispersion curve. The dispersion curve that was created at this site covered a wavelength range from approximately 1 m to 90 m. However, the internal consistency of the dispersion curve that was observed in the previous example was not apparent in this dispersion curve. The lack of overlap in the dispersion curve between different receiver spacings indicates a laterally variable profile over the extent of the SASW array. In this case, three possible theoretical dispersion curves were fit to the experimental dispersion curve, as shown in Figure 9b. The resulting shear wave velocity profiles are shown in Figure 10 and Tables 3a, 3b, and 3c. In this case a single value of  $V_{S30}$  could not be calculated, so a range of values based on the two deep profiles is presented in Table 5.

### ***Example 3: Shallow Profile***

At some remote locations it was not possible to use the bulldozer source to perform the SASW testing. Furthermore, in some cases the expanse of unobstructed land was not sufficient to perform the SASW test with the longest desired receiver spacings. Therefore, at these locations the measured dispersion curves contained energy with shorter wavelengths and the resulting shear wave velocity profiles did not penetrate to the desired depth of at least 30 m. The data collected from site LD-7 demonstrate this type of SASW result. Site LD-7 was located in a mountainous area in Golyaka. It was not possible to use the bulldozer source, so a drop-weight source was used to generate low frequency energy. The longest possible receiver spacing at this site was 15 m due to physical obstructions. The dispersion curve measured at LD-7 is presented in Figure 11a. There is some inconsistency between adjacent receiver spacings indicating slight lateral variability, but more importantly the maximum wavelength that could be measured at this site was 12 m. The theoretical fit to the experimental dispersion curve is presented in Figure 11b. The resulting shear wave velocity profile is presented in Figure 12 and Table 4. In this case, it was not possible to calculate  $V_{S-30}$  because the depth of penetration of the SASW measurement was not sufficient to develop a profile to 30m. At other sites where the shear wave velocity profile did not quite penetrate to 30 m, the shear wave profile was extrapolated to 30 m so that a  $V_{S-30}$  value could be estimated.



a. Experimental Dispersion Curve Measured with Six Receiver Spacings



b. Theoretical and Experimental Dispersion Curves

Figure 7 Experimental Dispersion Curve and Matching Theoretical Dispersion Curve from SASW Testing at the Ballica Afterstock Station

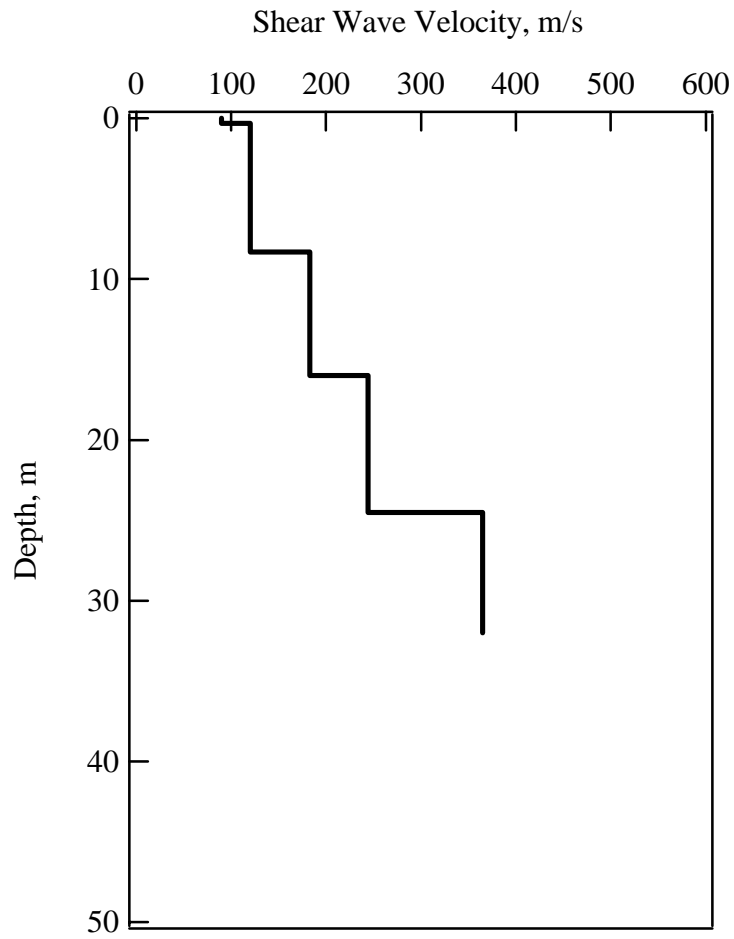


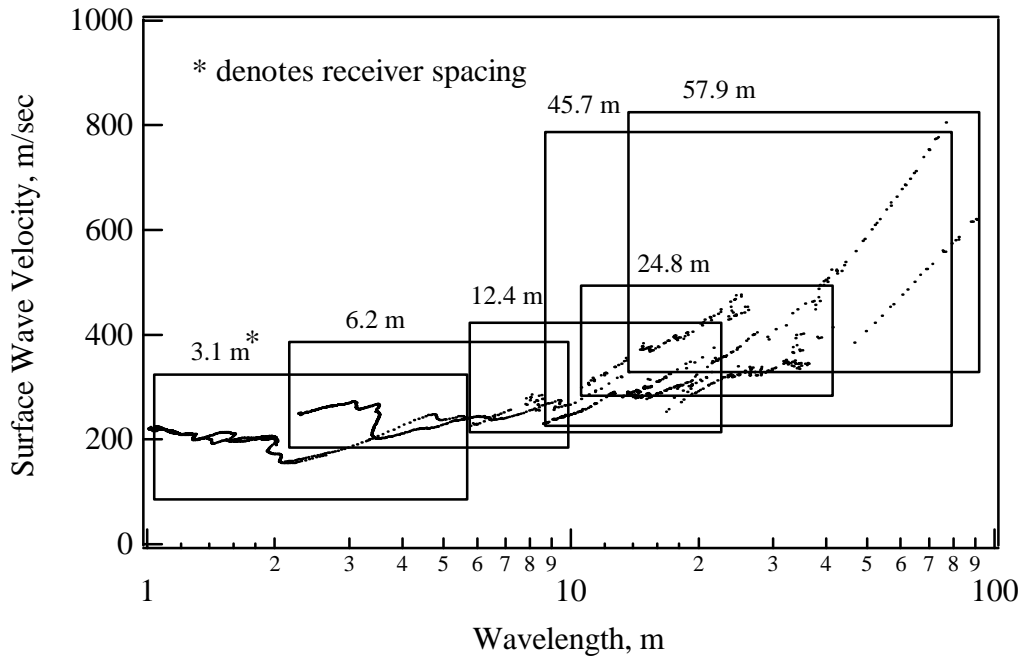
Figure 8 Shear Wave Velocity Profile at the Ballica (BAL) Site

Table 2: Tabulated Shear Wave Velocity Profile at the Ballica (BAL) Site

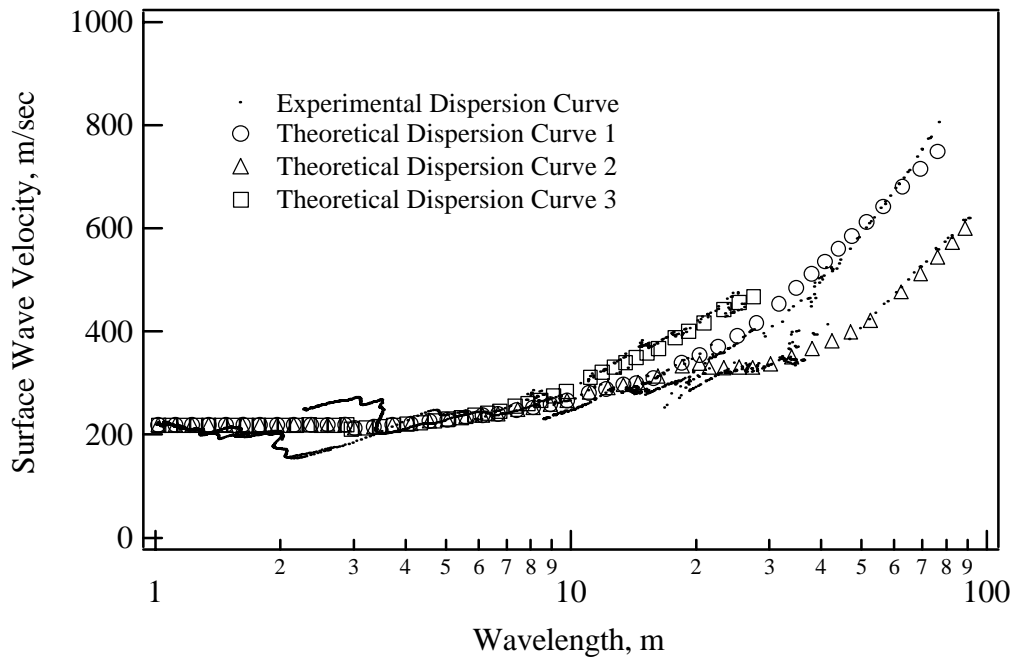
| Layer No. | Thickness, m | P-Wave Velocity, m/s | S-Wave Velocity, m/s | Poisson's Ratio | Mass Density, g/cc* |
|-----------|--------------|----------------------|----------------------|-----------------|---------------------|
| 1         | 0.3          | 179                  | 90                   | 0.33*           | 1.92                |
| 2         | 1.9          | 238                  | 120                  | 0.33*           | 1.92                |
| 3         | 6.1          | 1500*                | 120                  | 0.497**         | 1.92                |
| 4         | 7.6          | 1500*                | 186                  | 0.492**         | 1.92                |
| 5         | 7.6          | 1500*                | 244                  | 0.486**         | 1.92                |
| 6         | 9            | 1500*                | 365                  | 0.470**         | 1.92                |

\* assumed values

\*\* calculated from  $V_s$  and  $V_p = 1500$  m/s



a. Experimental Dispersion Curve Measured with Seven Receiver Spacings



b. Theoretical and Experimental Dispersion Curves

Figure 9 Experimental Dispersion Curve and Matching Theoretical Dispersion Curves from SASW Testing at the Arcelik (ARC) Strong-Motion Station

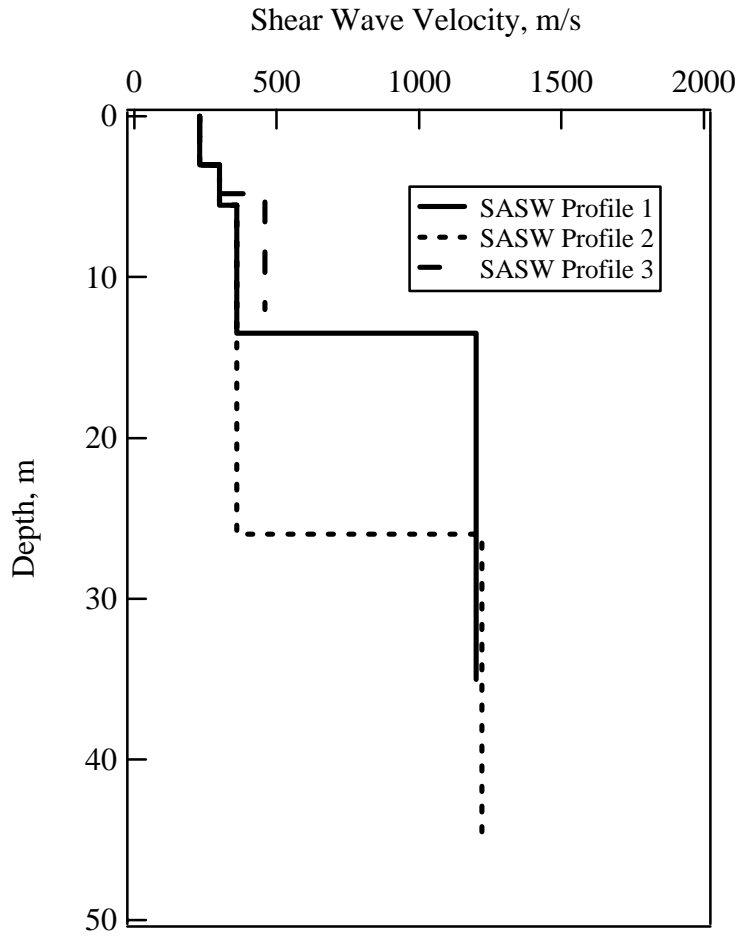


Figure 10 Shear Wave Velocity Profiles at the Arcelik (ARC) Site

Table 3a: Tabulated Shear Wave Velocity Profile at the Arcelik Site – Profile 1

| Layer No. | Thickness, m | P-Wave Velocity, m/s | S-Wave Velocity, m/s | Poisson's Ratio | Mass Density, g/cc* |
|-----------|--------------|----------------------|----------------------|-----------------|---------------------|
| 1         | 3.0          | 456                  | 230                  | 0.33*           | 1.92                |
| 2         | 2.5          | 1500*                | 300                  | 0.479**         | 1.92                |
| 3         | 8            | 1500*                | 360                  | 0.469**         | 1.92                |
| 4         | 21.5         | 2382                 | 1200                 | 0.33*           | 1.92                |

Table 3b: Tabulated Shear Wave Velocity Profile at the Arcelik Site – Profile 2

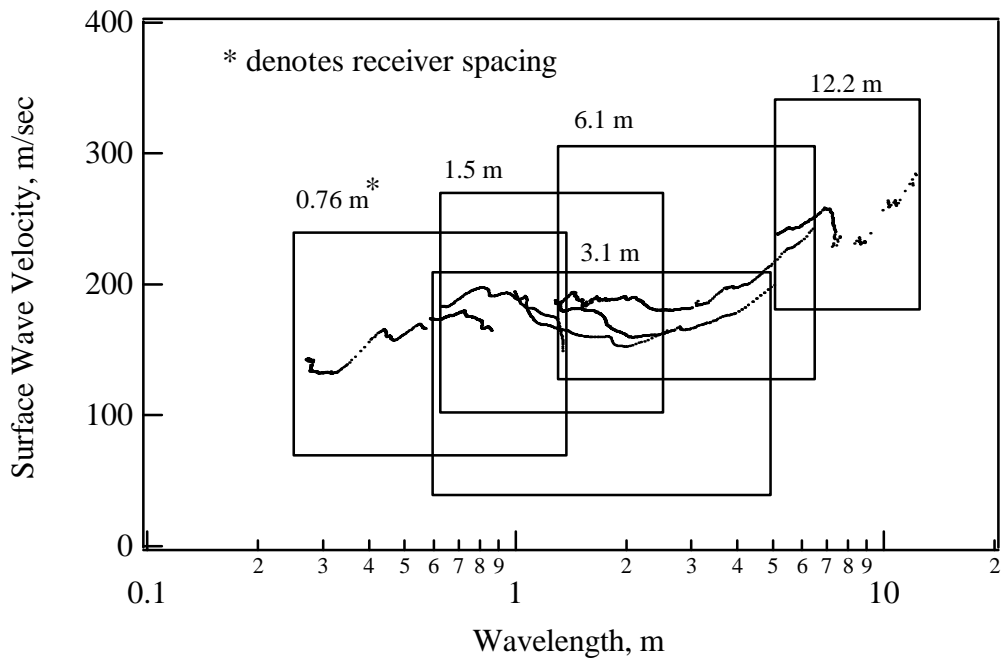
| Layer No. | Thickness, m | P-Wave Velocity, m/s | S-Wave Velocity, m/s | Poisson's Ratio | Mass Density, g/cc* |
|-----------|--------------|----------------------|----------------------|-----------------|---------------------|
| 1         | 3.0          | 445                  | 230                  | 0.33*           | 1.92                |
| 2         | 2.5          | 1500*                | 300                  | 0.479**         | 1.92                |
| 3         | 21           | 1500*                | 360                  | 0.469**         | 1.92                |
| 4         | 18.5         | 2422                 | 1220                 | 0.33*           | 1.92                |

Table 3c: Tabulated Shear Wave Velocity Profile at the Arcelik Site – Profile 3

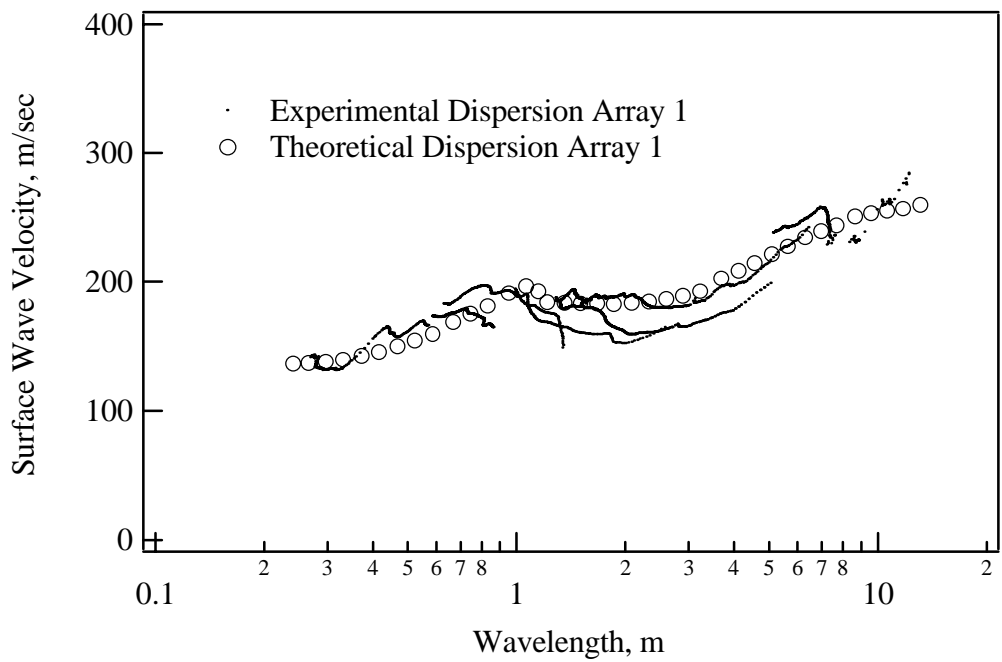
| Layer No. | Thickness, m | P-Wave Velocity, m/s | S-Wave Velocity, m/s | Poisson's Ratio | Mass Density, g/cc* |
|-----------|--------------|----------------------|----------------------|-----------------|---------------------|
| 1         | 3.0          | 456                  | 230                  | 0.33*           | 1.92                |
| 2         | 1.8          | 1500*                | 300                  | 0.479**         | 1.92                |
| 3         | 7.2          | 1500*                | 460                  | 0.448**         | 1.92                |

\* assumed values

\*\* calculated from  $V_s$  and  $V_p = 1500$  m/s



a. Experimental Dispersion Curve Measured with Five Receiver Spacings



b. Theoretical and Experimental Dispersion Curves

Figure 11 Experimental Dispersion Curve and Matching Theoretical Dispersion Curve from SASW Testing at the LD-7 Site

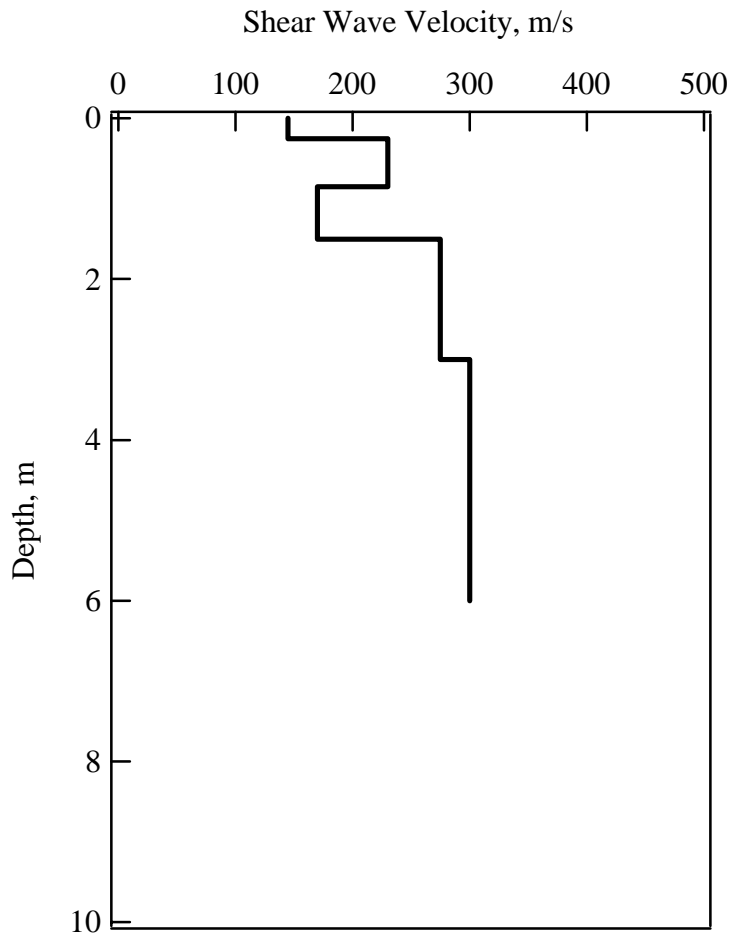


Figure 12 Shear Wave Velocity Profile at the LD-7 Site

Table 4: Tabulated Shear Wave Velocity Profile at the LD-7 Site

| Layer No. | Layer Thickness, m | P-Wave Velocity, m/s | S-Wave Velocity, m/s | Poisson's Ratio* | Mass Density, g/cc* |
|-----------|--------------------|----------------------|----------------------|------------------|---------------------|
| 1         | 0.25               | 288                  | 145                  | 0.33             | 1.92                |
| 2         | 0.6                | 456                  | 230                  | 0.33             | 1.92                |
| 3         | 0.6                | 338                  | 170                  | 0.33             | 1.92                |
| 4         | 1.5                | 546                  | 275                  | 0.33             | 1.92                |
| 5         | 3                  | 596                  | 300                  | 0.33             | 1.92                |

\*assumed values



## Experimental Results

In this section the shear wave velocity profiles for each station listed in Table 1 are presented. These shear wave velocity profiles are evaluated from forward modeling of the experimental field dispersion curves as discussed in the previous section. However, at some sites there are multiple interpretations of the dispersion curves as shown in Example 2 of the previous section. For these sites, the dispersion curves are shown and the multiple theoretical dispersion curves and resulting shear wave velocity profiles are presented and discussed. The experimental dispersion curves, theoretical dispersion curves and resulting shear wave velocity profiles at all 20 sites can be found in the Appendix of this report.

The SASW shear wave velocity profiles for each station are used to assign Geomatrix (1993) and Uniform Building Code (UBC, ICBO 1997) site classifications. The Geomatrix (1993) classification system includes rock or less than 5 m of soil (Class A), shallow soil less than 20 m thick (Class B), deep soil in narrow canyon with soil depth greater than 20m (Class C), deep soil in broad canyon with soil depth greater than 20m (Class D), and soft soil with a shear wave velocity less than 150 m/s (Class E). The UBC classification system is based on the average shear wave velocity over the top 30 m ( $V_{S-30}$ ) calculated using the travel time of a shear wave. The UBC site classification system includes hard rock ( $S_A$ ,  $V_{S-30}$  greater than 1500 m/s), rock ( $S_B$ ,  $V_{S-30}$  between 760 and 1500 m/s), very dense soil and soft rock ( $S_C$ ,  $V_{S-30}$  between 360 and 760 m/s), stiff soil ( $S_D$ ,  $V_{S-30}$  between 180 and 360 m/s), and soft soil ( $S_E$ ,  $V_{S-30}$  less than 180 m/s). A site also can be classified as soft soil if more than 3 m of soft clay is present. The Geomatrix classifications, UBC classifications, and  $V_{S-30}$  values are discussed for each site and also listed in Table 2 at the end of this section.

### *Arcelik*

The Arcelik (N 40.8236, E29.3607) station is located in the half-basement of a 2-story, reinforced concrete structure. This structure is located on the Arcelik industrial facility grounds north of Gebze. The topography of the area is gently rolling hills. Hammers and a bulldozer were used as wave sources and the SASW array was located approximately 60 m from the strong motion station.

The experimental dispersion data are shown in Figure 9a. At wavelengths greater than 10 m, the dispersion data diverge into three separate curves. These data are from different receiver spacings and are assumed to be the result of lateral variability at the site, as discussed previously. One of the advantages of the global measurements obtained from SASW testing is that the data from different receiver spacings give an indication of lateral variability. Three theoretical dispersion curves fit to these data are shown in Figure 9b and the resulting shear wave velocity profiles are shown in Figure 10. The data show velocities less than 500 m/s in the top 10 m, with an increase to over 1000 m/s at a depth between 15 and 25 m. The Arcelik station is considered a shallow soil site (Class B) in the Geomatrix classification system, with less than about 20 m of soil. Using profiles 1 or 2,  $V_{S-30}$  for this site is either 500 or 360 m/s. Based on the UBC classification system, this site is a soft rock/dense soil site ( $S_C$ ).

### *Ambarli*

The Ambarli (N 40.9809, E28.6926) station is located in the lowest level of a 2-story, reinforced concrete structure. This structure is located on the grounds of a power generation plant in western Istanbul. The facility is located in an alluvial valley, less than 5 km wide.

Hammers and a bulldozer were used as wave sources and the SASW array was located approximately 25 m from the strong motion station.

The experimental and theoretical dispersion curves are shown in the appendix along with the tabulated  $V_s$  profile. The shear wave velocity profile from the SASW testing is shown in Figure 13, along with a shear wave velocity profile from Kudo et al. (2001). The SASW data show velocities below 200 m/s extending to a depth of 25 m. Even at a depth of 40 m the shear wave velocity is only 350 m/s. These low velocities explain the large ground motions recorded at Ambarli. The Kudo et al. (2001) profile was developed from inversion of surface wave energy generated by microtremors. Microtremor motions have significant low-frequency energy, but are deficient in high-frequency energy needed to evaluate near-surface material. Consequently, microtremor  $V_s$  profiles can provide accurate data at depth, but cannot resolve the layering at shallow depths. The SASW and microtremor profiles in Figure 13 agree at depth, but only SASW can resolve the low-velocity layers near the ground surface. This site is considered a soft soil site (Class E) in the Geomatrix classification system. The  $V_{s-30}$  for this site is 175 m/s, making it also a soft soil site ( $S_E$ ) in the UBC classification system. It is important to note that using the microtremor shear wave velocity profile to classify this site would result in incorrect classifications, Class D for Geomatrix and  $S_D$  for UBC.

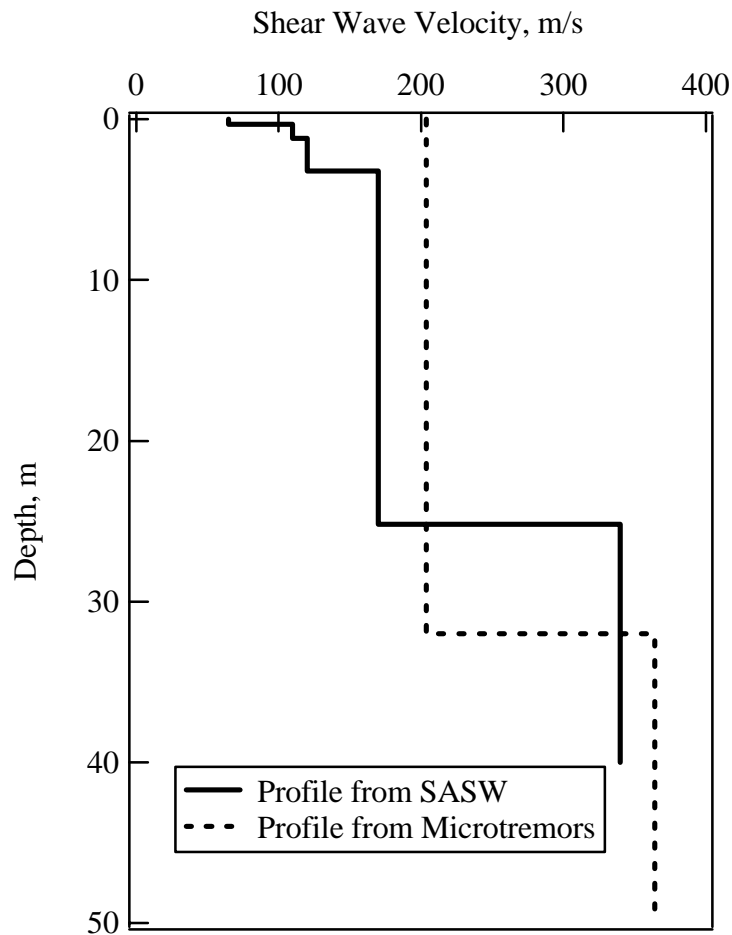


Figure 13 Shear Wave Velocity Profile Determined from SASW and Microtremor Arrays at Ambarli (ATS)

### **Bolu**

The Bolu (N 40.7460, E31.6071) station is located in the lowest level of a 1 story, reinforced concrete structure. However, this structure is part of a campus of several buildings of various heights and is adjacent to a multi-story structure that was damaged during the Duzce earthquake. The structure is located in the large Bolu alluvial basin. Significant tension cracks were observed at the site, indicating clayey soil. Hammers and a bulldozer were used as wave sources and the SASW array was located approximately 150 m from the strong motion station.

The experimental and theoretical dispersion curves from Bolu are shown in Figure 14 and the resulting shear wave velocity profile from SASW testing is shown in Figure 15. The dispersion data are consistent between receiver spacings, in contrast to the dispersion data from Arcelik shown in Figure 9a. The shear wave velocity profile (Figure 15) indicates that the top 15 m of the site consists of material with  $V_s$  less than 300 m/s. At a depth of 40 m, the shear wave velocity reaches about 400 m/s. This site is considered a deep soil site (Class D) in the Geomatrix classification system. The  $V_{S-30}$  for this site is 290 m/s, making it a stiff soil site ( $S_D$ ) in the UBC classification system.

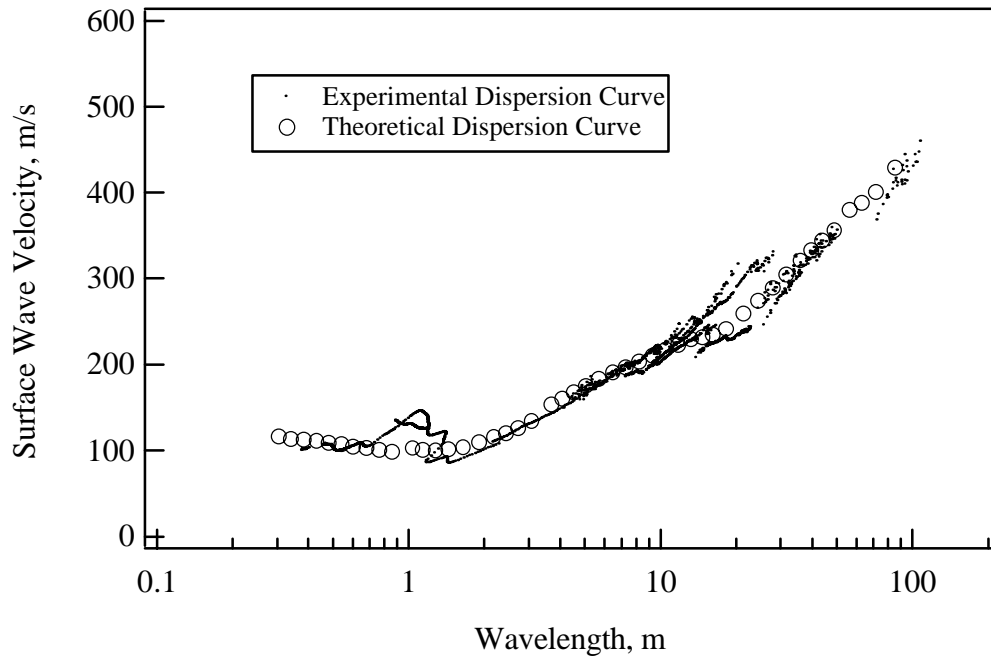


Figure 14 Theoretical and Experimental Dispersion Curves from SASW testing at Bolu (BOL)

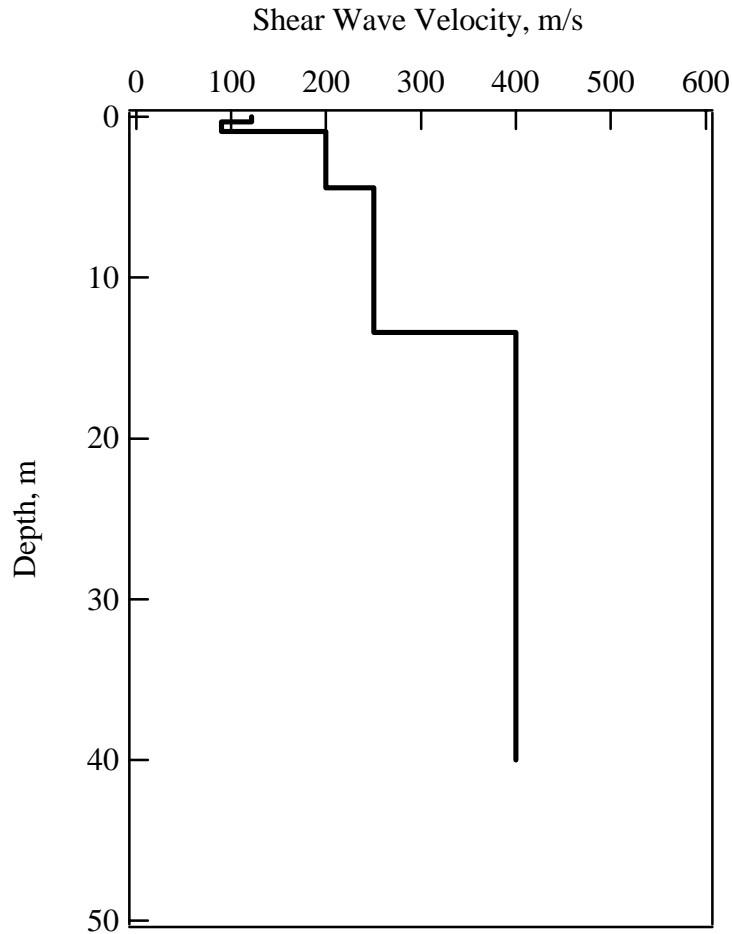


Figure 15 Shear Wave Velocity Profile Determined from SASW Testing at Bolu (BOL)

### ***Cekmece***

The Cekmece (N 41.0238, E28.7594) station is located in the lowest level of a 1-story, reinforced concrete structure. The structure is located on the campus of a nuclear research facility in western Istanbul. The facility is located at the top of a broad hill. Significant tension cracks were observed at the site, indicating clayey soil. Hammers and a bulldozer were used as wave sources and the SASW array was located approximately 60 m from the strong motion station.

The experimental and theoretical dispersion curves are shown in the appendix along with the tabulated  $V_S$  profile. The shear wave velocity profile from SASW testing is shown in Figure 16, along with a shear wave velocity profile from Kudo et al. (2001). The SASW profile indicates that the velocity of the near-surface materials is less than 200 m/s, but the velocity quickly increases to 600 m/s at a depth of 15 m. The Kudo et al. (2001) and SASW curves agree at depths below about 15 m, but the microtremor data cannot capture the variation in shear wave velocity near the surface. However, the shear wave velocity in the top 15 m from microtremor measurements agrees with the average velocity in this depth range from SASW testing. This site is somewhat difficult to classify because the velocity reaches 600 m/s at a depth of 15 m. If one

considers this layer as rock, then this station is considered a shallow soil site. However, rock is typically identified as material with a velocity greater than about 750 m/s. Based on the microtremor profile, this velocity is not reached until a depth of about 45 m, making this site a deep soil site (Class D) in the Geomatrix classification system. The  $V_{S-30}$  for this site is 350 m/s, making it a stiff soil site ( $S_D$ ) in the UBC classification system.

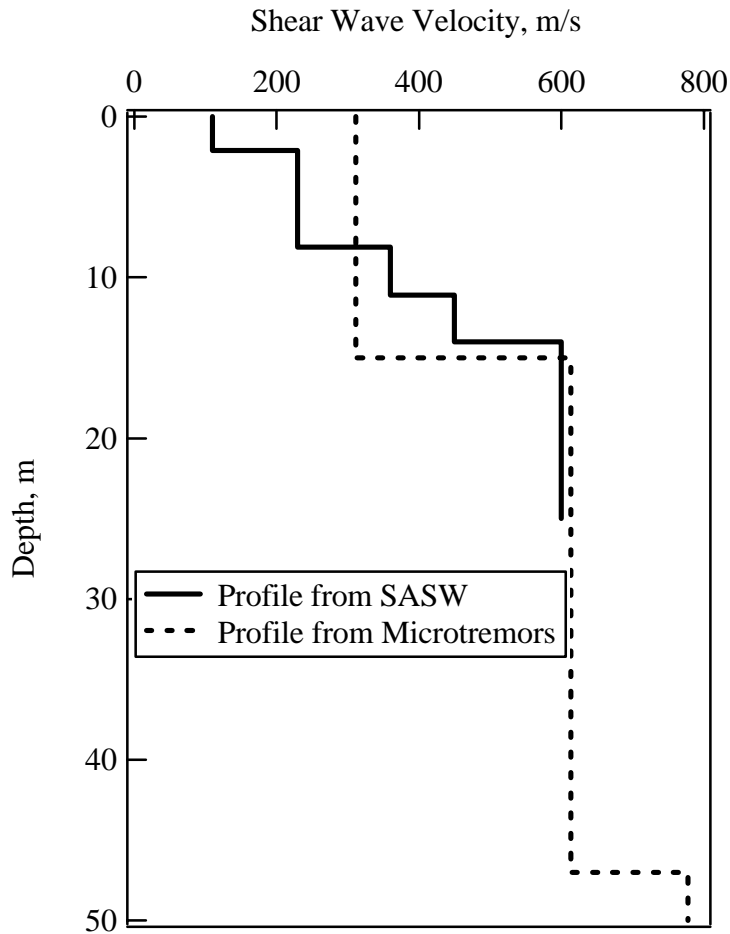


Figure 16 Shear Wave Velocity Profile Determined from SASW and Microtremor Arrays at Cekmece (CNA)

### *Duzce*

The Duzce (N 40.8437, E31.1489) station is located in the lowest level of a 1-story, reinforced concrete structure. The structure is located in the middle of the city and lies in the large Duzce alluvial basin. Hammers and a bulldozer were used as the wave sources and the SASW array was located approximately 15 m from the strong motion station..

The experimental and theoretical dispersion curves are shown in the appendix along with the tabulated  $V_S$  profile. The shear wave velocity profile from SASW testing is shown in Figure 17, along with a shear wave velocity profile from Kudo et al. (2001). The SASW profile indicates that the velocity of the near-surface materials is less than 200 m/s, but the velocity quickly increases to 400 m/s at 15 m. The Kudo et al. (2001) profile shows a constant shear wave

velocity of 260 m/s extending from the surface to a depth of 35 m. This value agrees with the average SASW value of the same depth range, but it does not capture the shear wave velocity variation in this zone. At depths below about 40 m, both profiles show a shear wave velocity between 400 and 450 m/s. This site is considered a deep soil site (Class D) in the Geomatrix classification system. The  $V_{S-30}$  for this site is 275 m/s, making it a stiff soil site ( $S_D$ ) in the UBC classification system.

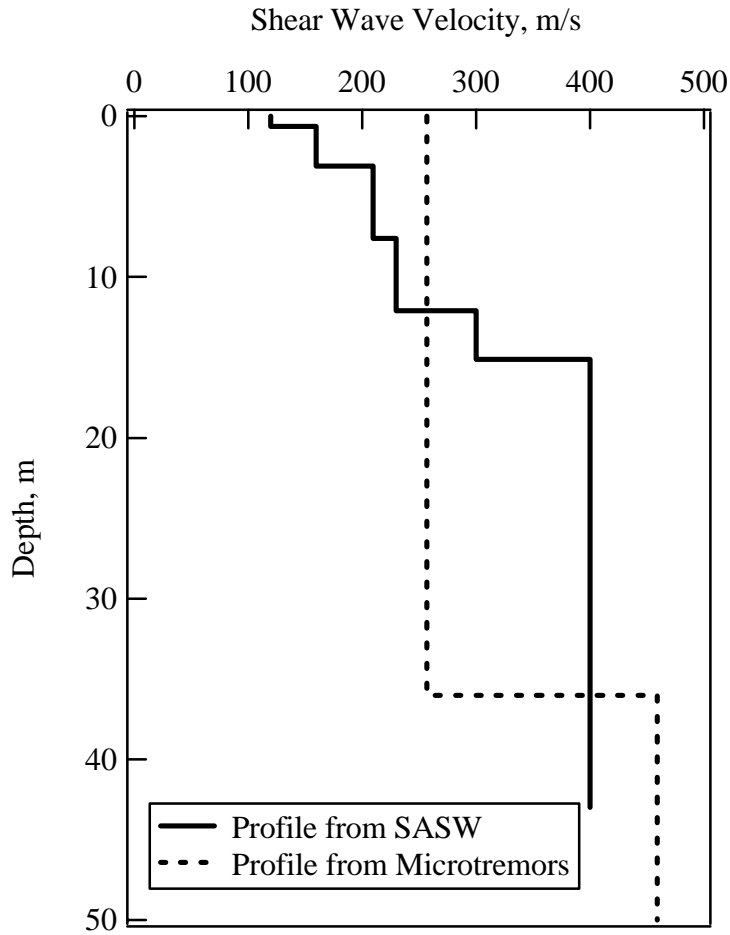


Figure 17 Shear Wave Velocity Profile Determined from SASW and Microtremor Arrays at Duzce (DZC)

### **Gebze**

The Gebze (N 40. 8627, E29.4494) station is located in the half basement of a 4-story, reinforced concrete structure that was damaged during the Izmit earthquake. The structure is located at the Tubitak Marmara Research Center in Gebze. The topography in the area is rolling hills. Hammers and a bulldozer were used as wave sources and the SASW array was located approximately 60 m from the strong motion station.

The experimental and theoretical dispersion curves are shown in the appendix along with the tabulated  $V_S$  profile. The shear wave velocity profile from SASW testing is shown in Figure 18. A very thin layer of soft material is found at the surface ( $V_S$  less than 200 m/s), but the shear wave velocity very quickly reaches 1000 m/s at a depth of 4 m. This is one of the stiffest sites tested as part of this study and the site is considered a rock site (Class A) in the Geomatrix classification system. The  $V_{S-30}$  for this site is 750 m/s, making it a rock site ( $S_B$ ) in the UBC classification system.

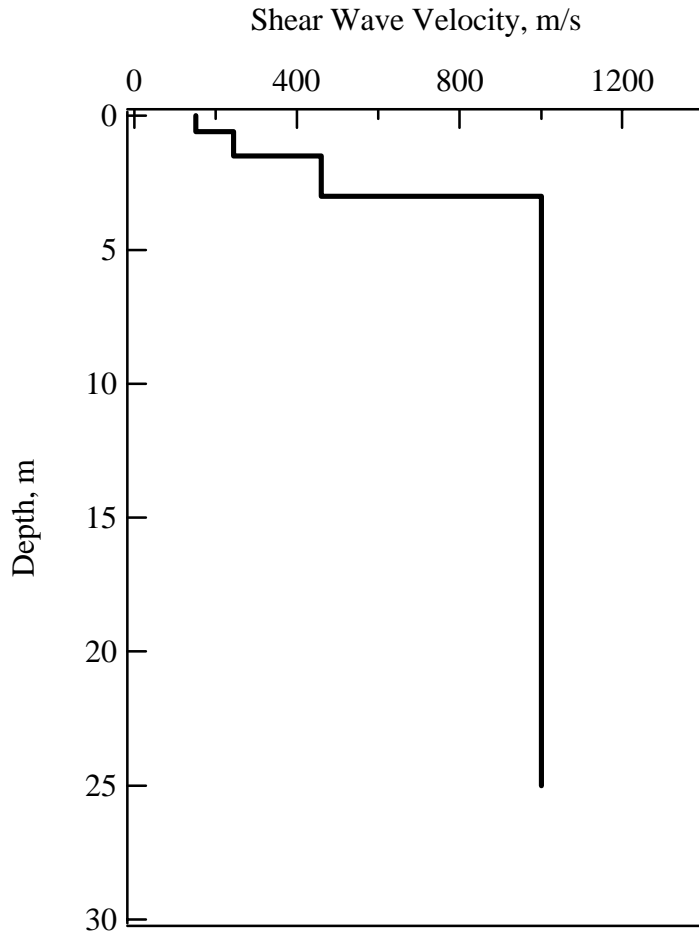


Figure 18 Shear Wave Velocity Profile Determined from SASW Testing at Gebze (GBZ)

***Iznik***

The Iznik (N 40.4416, E29.7172) station is located in the lowest level of a 1-story, masonry structure near the eastern edge of Lake Iznik. The structure is located at the highway department maintenance facility in Iznik. The geology of this area indicates the station is located on Holocene alluvium around the edge of Lake Iznik. Hammers and a drop weight were used as

wave sources and the SASW array was located approximately 15 m from the strong motion station.

The experimental and theoretical dispersion curves are shown in the appendix along with the tabulated  $V_S$  profile. The experimental dispersion data for Iznik are shown in Figure 19. The data below wavelengths of 8 m are consistent, but the surface wave velocities at longer wavelengths are scattered and lower than the values in the wavelength range of 6 to 8 m. These data indicate a stiff layer underlain by a softer layer. The theoretical dispersion curve is shown in Figure 19 and matches the experimental data relatively well. The corresponding shear wave velocity profile is shown in Figure 20. In the top 15 m, the shear wave velocity of the soil is generally below 200 m/s. However, at a depth of 2.5 m there is a 1.5 m-thick layer of stiffer material with a shear wave velocity greater than 350 m/s. This is a difficult site to classify because the shear wave velocity profile only extends to a depth of 15 m. However, because the geology indicates that this is an alluvial plane, this site is considered a deep soil site (Class D) in the Geomatrix classification system. If the shear wave velocity at 15 m is extended to 30 m a lower bound  $V_{S-30}$  can be calculated. For this case,  $V_{S-30}$  is 190 m/s if we include the stiff layer and 180 m/s if we ignore it. Consequently, this site can be classified as either a stiff soil site ( $S_D$ ) or soft soil site ( $S_E$ ) in the UBC classification system.

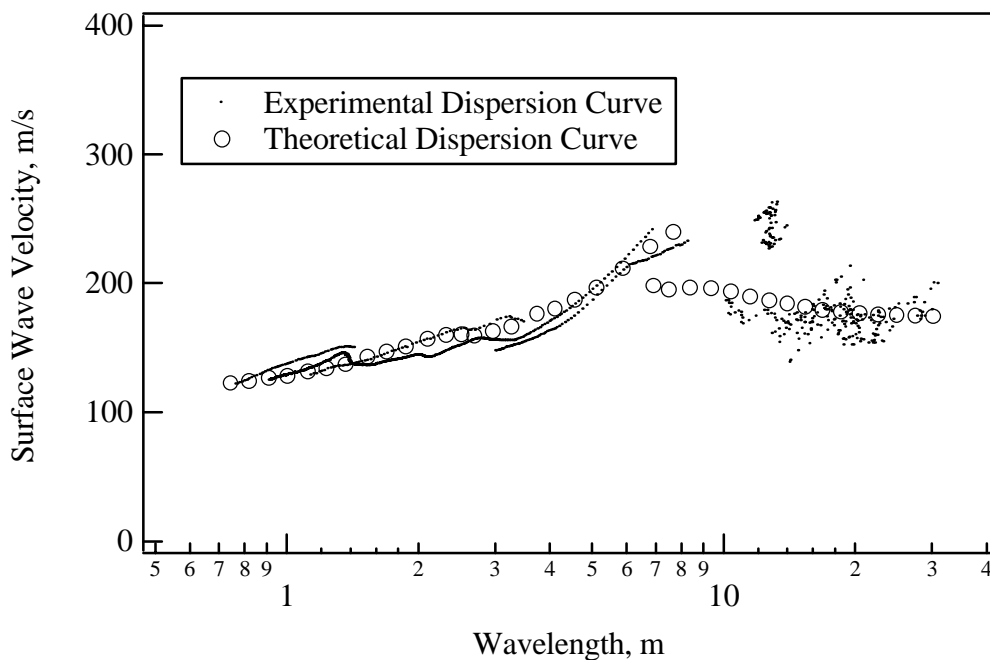


Figure 19 Theoretical and Experimental Dispersion Curves from SASW testing at Iznik (IZN)



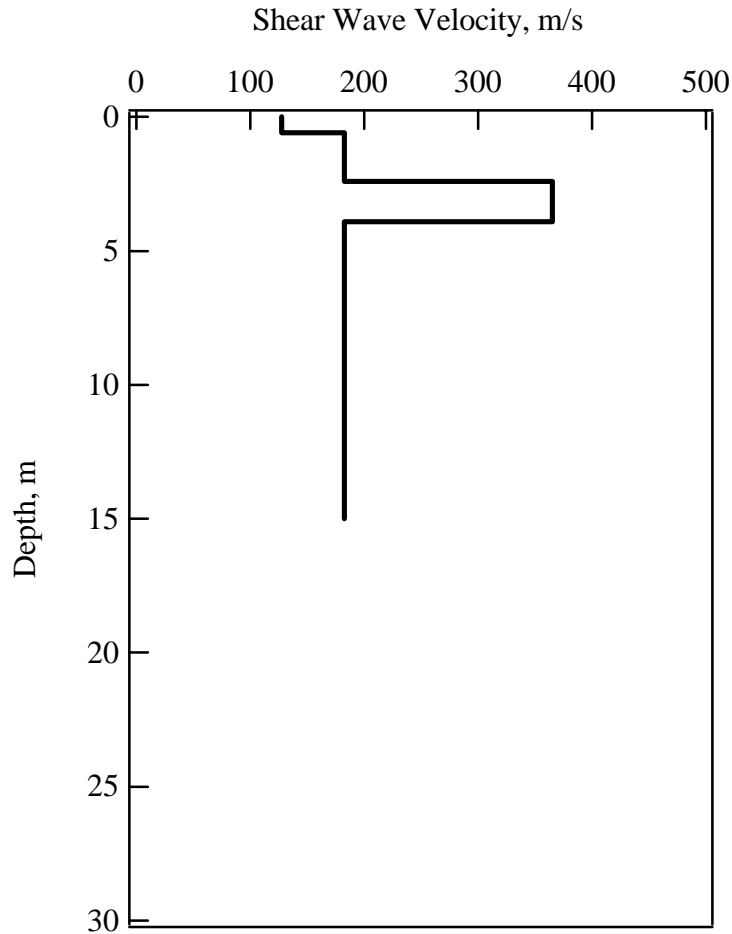


Figure 20 Shear Wave Velocity Profile Determined from SASW Testing at Iznik (IZN)

### *Izmit*

The Izmit (N 40.7664, E29.9175) station is located in the lowest level of a 3-story, reinforced concrete structure. The structure is located in the hills north of Izmit Bay in the city of Izmit. Hammers and a drop weight were used as wave sources and the SASW array was located approximately 25 m from the strong motion station.

The experimental and theoretical dispersion curves are shown in the appendix along with the tabulated  $V_S$  profile. The shear wave velocity profile from SASW testing is shown in Figure 21. Two shear wave velocity profile interpretations are shown in Figure 21, but both show similar trends. Both profiles show a thin 250 m/s layer near the surface underlain by significantly stiffer material. The shear wave velocity quickly increases to 1500 m/s at a depth of 10 m. This is the stiffest site tested as part of this study and the site is considered a rock site (Class A) in the Geomatrix classification system. Extrapolating the velocity profile to 30 m, the  $V_{S-30}$  for this site is 800 m/s, making it also a rock site ( $S_B$ ) in the UBC classification system.

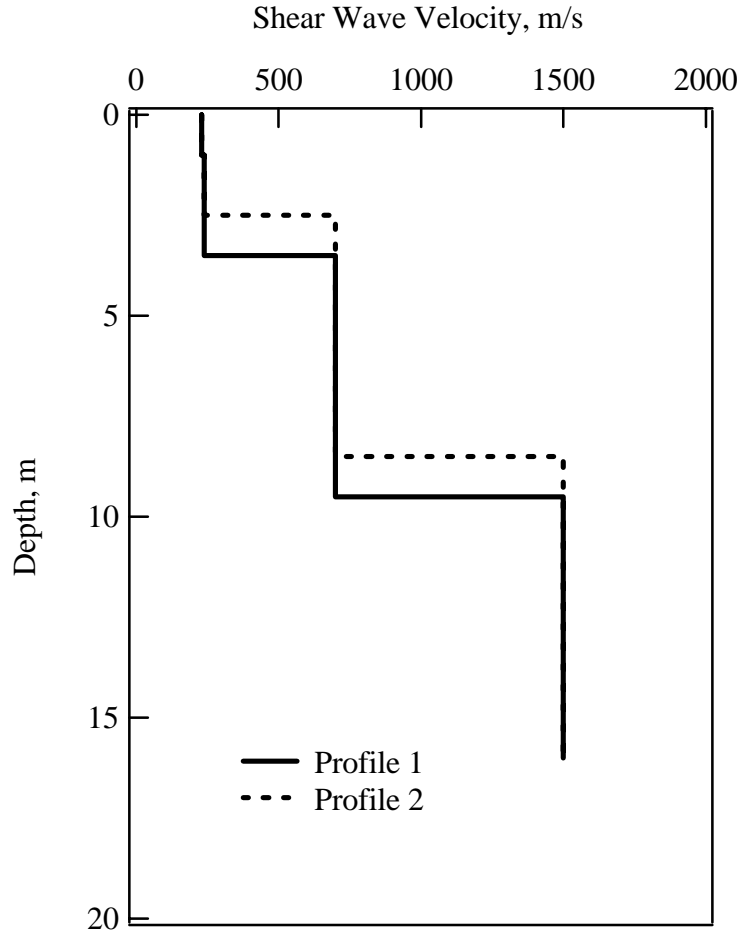


Figure 21 Shear Wave Velocity Profile Determined from SASW Testing at Izmit (IZT)

### ***Sakarya***

The Sakarya (N 40.7664, E29.9175) station is located in the lowest level of a 1-story structure of lightweight construction. The structure is located on a hill in the southwest part of Adapazari. It is important to note that this station is not located on the soft sediments in the central part of Adapazari. Hammers and a drop weight were used as wave sources and the SASW array was located approximately 7.5 m from the strong motion station. It was difficult to use large receiver spacings at this station because many temporary structures were built in the area after the Izmit earthquake.

The experimental dispersion data from Sakarya are shown in Figure 22. Between wavelengths of 4 m and 30 m the data indicate several different possible dispersion curves. The data in this area are from different receiver spacings and may be the result of lateral variability at the site. The source of this variability may be the location of the site at the crest of a hill, where the weathered zone may vary. Two theoretical dispersion curves fit to the upper and lower bounds of these data are shown in Figure 22, and the resulting shear wave velocity profiles are shown in Figure 23. The profiles show a very thin low velocity layer near the surface, and the velocity reaches 900 m/s at a depth between 5 and 15 m. For comparison, the microtremor shear

wave velocity profile from Kudo et al. (2000) is shown in Figure 23. This profile shows a constant velocity of about 1000 m/s, which agrees with the deeper SASW measurements. This station is considered a shallow soil site (Class B) in the Geomatrix classification system, with less than 20 m of soil. Using profile 1 extended to 30 m, the  $V_{S-30}$  for this site is 470 m/s, making it a soft rock/dense soil site ( $S_C$ ) in the UBC classification system.

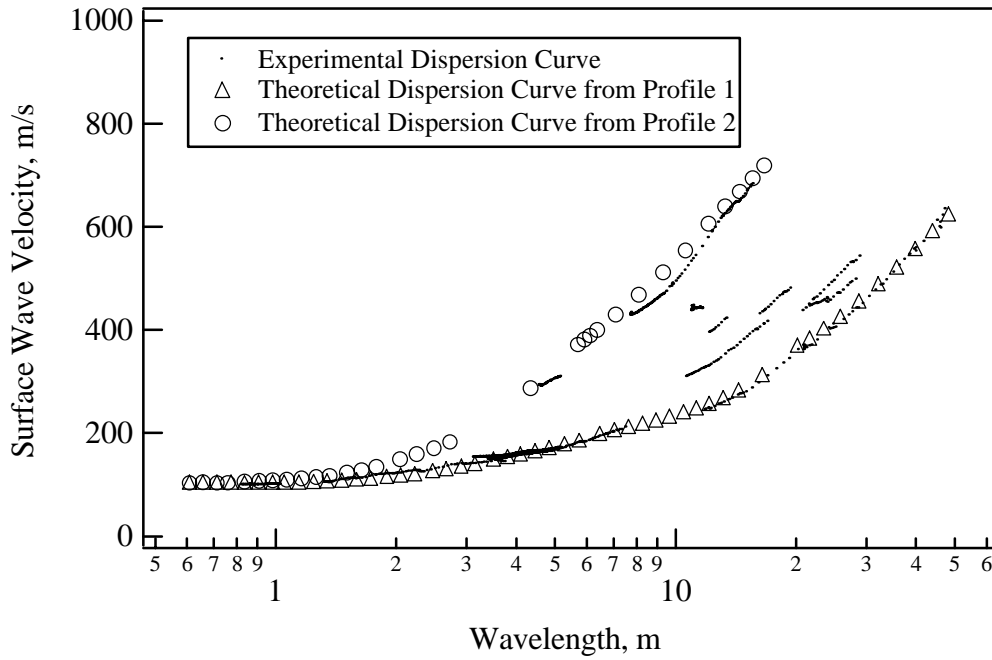


Figure 22 Theoretical and Experimental Dispersion Curves from SASW testing at Sakarya (SKR)

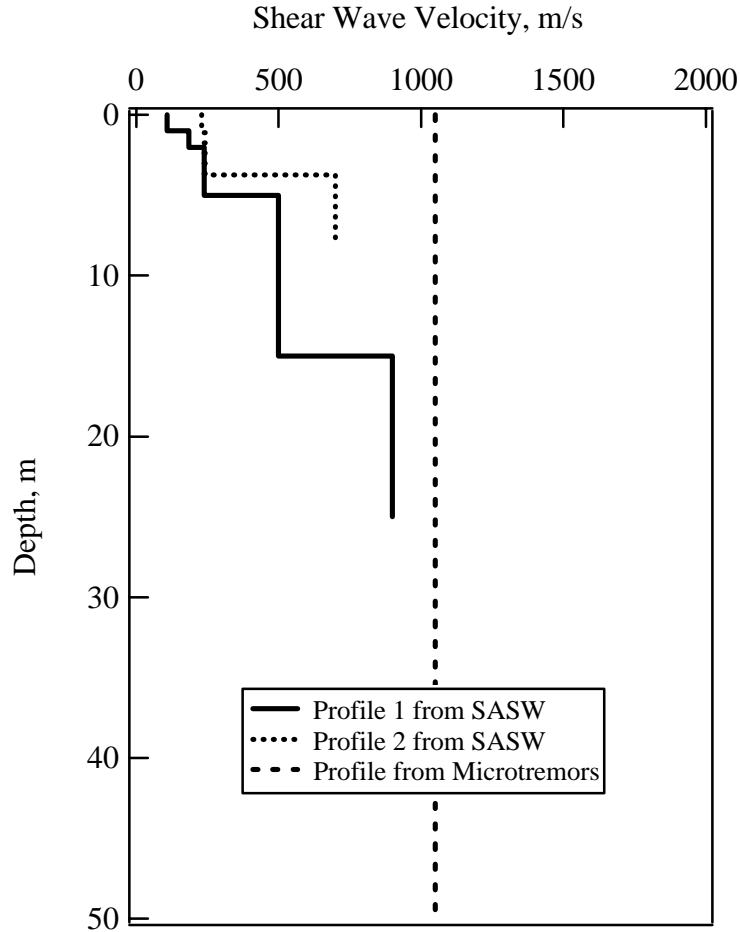


Figure 23 Shear Wave Velocity Profile Determined from SASW and Microtremor Arrays at Sakarya (SKR)

### *Yarimca*

The Yarimca (N 40.7639, E29.7620) station is located in the lowest level of a 3-story reinforced concrete structure found on the grounds of the Yarimca Petkim Refinery. The structure is located on an alluvial plane on the northern margin of Izmit Bay. Hammers and a bulldozer were used as wave sources and the SASW array was located approximately 30 m from the strong motion station.

The experimental and theoretical dispersion curves are shown in the appendix along with the tabulated  $V_S$  profile. The shear wave velocity profile from SASW testing is shown in Figure 24, along with a microtremor shear wave velocity profile from Kudo et al. (2001). Both profiles show a relatively constant shear wave velocity of between 300 and 350 m/s in the top 40 m. The SASW profile also shows a 3 m-thick layer near the surface with a low velocity of 200 m/s. This site is considered a deep soil site (Class D) in the Geomatrix classification system. The  $V_{S-30}$  for this site is 300 m/s, making it a stiff soil site ( $S_D$ ) in the UBC classification system.

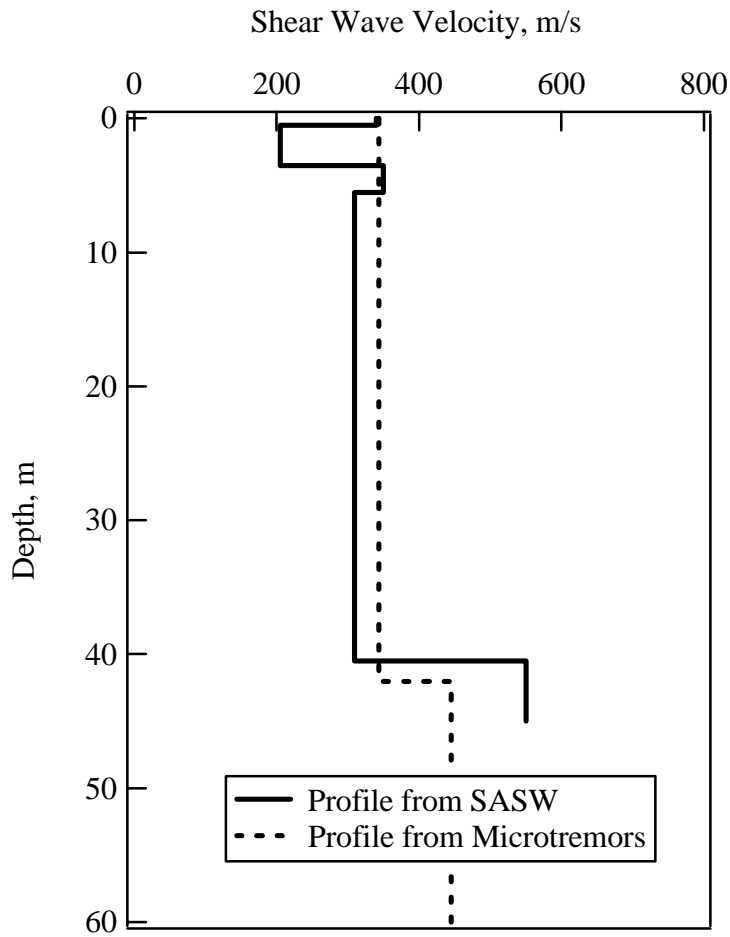


Figure 24 Shear Wave Velocity Profile Determined from SASW and Microtremor Arrays at Yarimca (YPT)

### ***LD-3***

The LD-3 (N 40.6698, E30.6655) station was a temporary station located in a small, empty water tank. The water tank was buried in the side of hill which showed signs of weathering. SASW testing was performed on a road cut below the actual location of the station. Only hammers were used as wave sources and the SASW array was located approximately 30 m from the strong motion station.

The experimental and theoretical dispersion curves are shown in the appendix along with the tabulated  $V_S$  profile. The shear wave velocity profile from SASW testing is shown in Figure 25. Because only hammers were used as wave sources, the shear wave velocity profile only extends to a depth of 15 m. The profile shows that the velocity reaches a value of 550 m/s at a depth of 5 m. Because of the hilly topography of the site and the relatively large velocity measured at 5 m, this site is considered a shallow soil site (Class B) in the Geomatrix classification system. If the shear wave velocity at 15 m is extended to 30 m, a lower bound  $V_{S-30}$  can be calculated. For this

case,  $V_{S-30}$  is 520 m/s, making this site a soft rock/dense soil site ( $S_C$ ) in the UBC classification system.

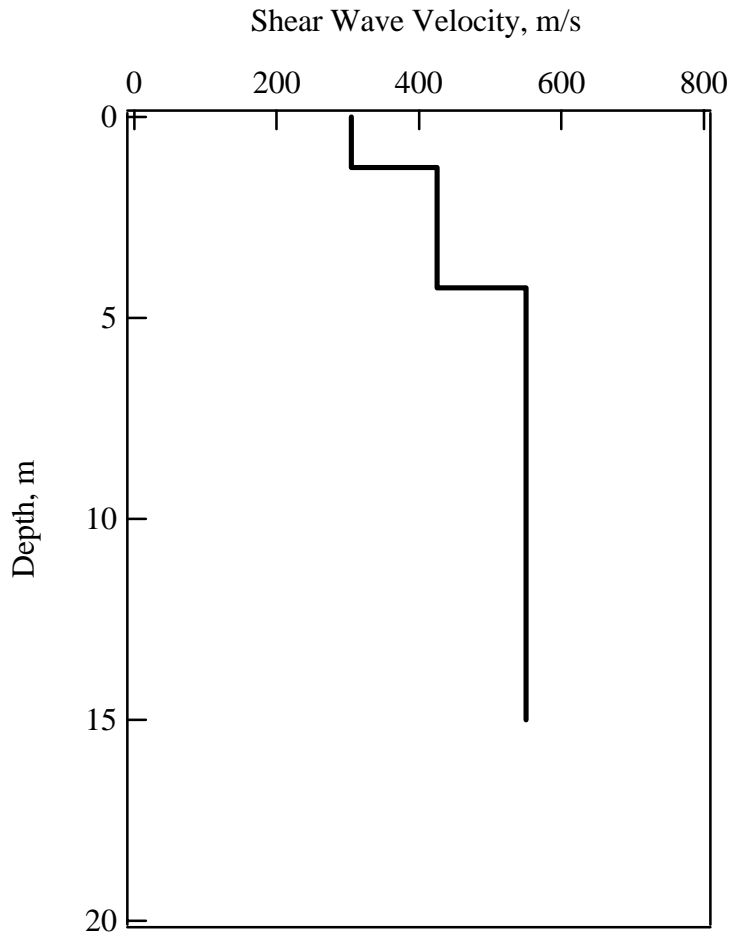


Figure 25 Shear Wave Velocity Profile Determined from SASW Testing at LD3

**LD-5**

The LD-5 (N 40.7025, E30.8552) station was a temporary station located in the free field in a mountainous area between Akyazi and Duzce. SASW testing was performed on a road cut below the actual location of the station. Hammers and a drop weight were used as wave sources and the SASW array was located approximately 25 m from the strong motion station.

The experimental and theoretical dispersion curves are shown in the appendix along with the tabulated  $V_S$  profile. The shear wave velocity profile from SASW testing is shown in Figure 26. The shear wave velocity at the surface is about 200 m/s, but it quickly reaches 750 m/s at a depth of about 5 m. This site is considered a rock site (Class A) in the Geomatrix classification system. If the shear wave velocity at 17 m is extended to 30m, a lower bound  $V_{S-30}$  can be calculated. For this case,  $V_{S-30}$  is 660 m/s, making this site a soft rock/dense soil site ( $S_C$ ) in the UBC classification system

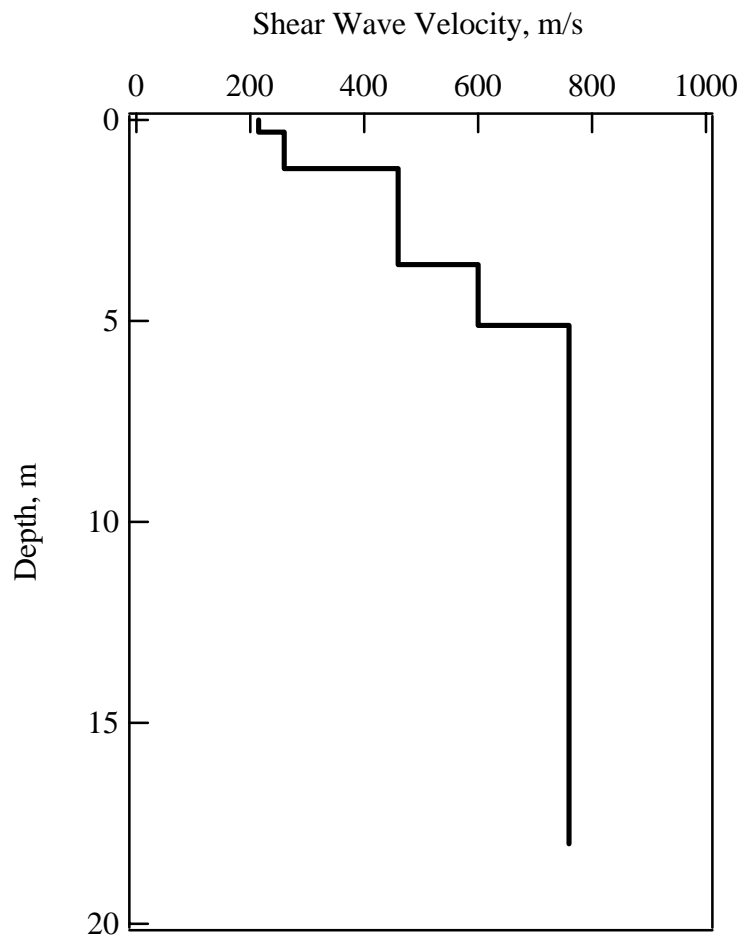


Figure 26 Shear Wave Velocity Profile Determined from SASW Testing at LD-5

### ***LD-7***

The LD-7 (N 40.7552, E31.0148) station was a temporary station located in the free field in a mountainous area south of Eften Lake. SASW testing was performed on a driveway cut below the actual location of the station. Hammers and a drop weight were used as wave sources and the SASW array was located approximately 25 m from the strong motion station.

The experimental and theoretical dispersion curves are shown in the appendix along with the tabulated  $V_S$  profile. The shear wave velocity profile from SASW testing is shown in Figure 12. Because of limited space for long receiver spacings, the shear wave velocity profile extends only 6 m. Over this depth, the shear wave velocity never exceeds 300 m/s. Because of the limited depth of profiling at this site, judgment must be employed to evaluate the site classification. Based on the mountainous topography in this area, this site is considered a shallow soil site (Class B) in the Geomatrix classification system, with less than 20 m of soil. Because the shear wave velocity profile extends only to 6 m, the profile was not extended to 30 m to calculate  $V_{S-30}$ . Therefore, a UBC site class cannot be evaluated for this site.

### ***LD-9***

The LD-9 (N 40.7773, E30.6127) station was a temporary station located in the free field on a hill in the middle of the large Sakarya alluvial valley, east of Adapazari. SASW testing was performed on a road cut significantly below the actual location of the station (i.e. 15-m elevation difference) because it was not possible logistically to perform the test at the actual station location. Hammers and a drop weight were used as wave sources and the SASW array was located approximately 75 m from the strong motion station.

The experimental and theoretical dispersion curves are shown in the appendix along with the tabulated  $V_S$  profile. The shear wave velocity profiles from SASW testing are shown in Figure 27. Profile 1 is from testing along a road cut, while Profile 2 is from testing along a road near the base of the hill. The elevation difference between Profiles 1 and 2 was only about 3 m, and both were significantly below the actual location of the station. Both profiles show a velocity of about 550 to 600 m/s at a depth of 5 m. Profile 1 indicates a 5-m thick layer near the surface with velocities less than 400 m/s, but this layer may be a result of the road cut/fill. Profile 2 shows that the velocity reaches 1200 m/s at a depth of 10 m. Unfortunately, the depth to this high velocity layer at the actual station location is unknown. Based on these measurements and judgment, this site is considered a shallow soil site (Class B) in the Geomatrix classification system. Using the two shear wave velocity profiles from this site,  $V_{S-30}$  is estimated between 500 and 800 m/s. These values indicate the site is either a soft rock/dense soil site ( $S_C$ ) or a rock site ( $S_B$ ) in the UBC classification system.



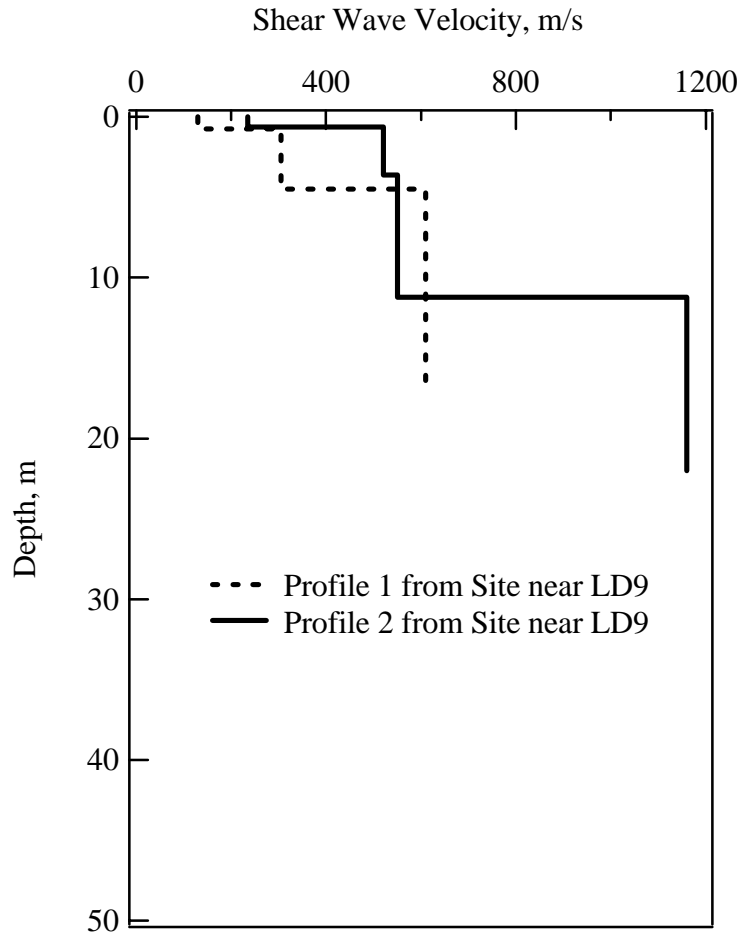


Figure 27 Shear Wave Velocity Profile Determined from SASW Testing at LD-9

**LD-10**

The LD-10 (N 40.7202, E30.7922) station was a temporary station located in the free field in a mountaineous area between Akyazi and Duzce. SASW testing was performed in an apple orchard on the side of a hill. Hammers and a drop weight were used as wave sources and the SASW array was located more than 150 m from the strong motion station.

The experimental and theoretical dispersion curves are shown in the appendix along with the tabulated  $V_S$  profile. The shear wave velocity profile from SASW testing is shown in Figure 28. A very thin layer of low velocity material is found at the surface, but the velocity quickly increases to 800 m/s at a depth of 12 m. This site is considered a shallow soil site (Class B) in the Geomatrix classification system. The  $V_{S-30}$  for this site is 480 m/s, making it a soft rock/dense soil site ( $S_C$ ) in the UBC classification system.

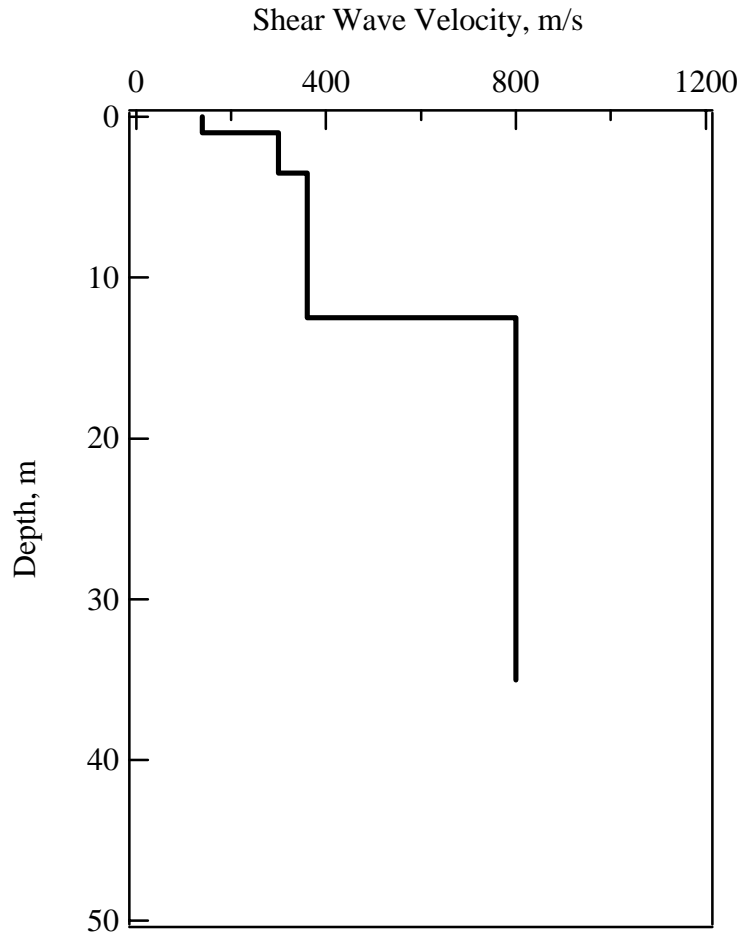


Figure 28 Shear Wave Velocity Profile Determined from SASW Testing at LD-10

***LD-12***

The LD-12 (N 40.7228, E30.8200) station was a temporary station located in the free field in a mountaineous area between Akyazi and Duzce. SASW testing was performed in a field located at the base of a steeper hill. Hammers and a drop weight were used as wave sources and the SASW array was located approximately 90 m from the strong motion station.

The experimental and theoretical dispersion curves are shown in the appendix along with the tabulated  $V_S$  profile. The shear wave velocity profile from SASW testing is shown in Figure 29. A very thin 100 m/s layer is indicated near the surface, but the velocity reaches 300 m/s at 10 m and 670 m/s at 18 m. Although 670 m/s is not quite large enough to be considered rock, there is a significant impedance/velocity contrast at 18 m. Consequently, this site is considered a shallow soil site (Class B) in the Geomatrix classification system. The  $V_{S-30}$  for this site is 340 m/s, making it a stiff soil site ( $S_D$ ) in the UBC classification system.

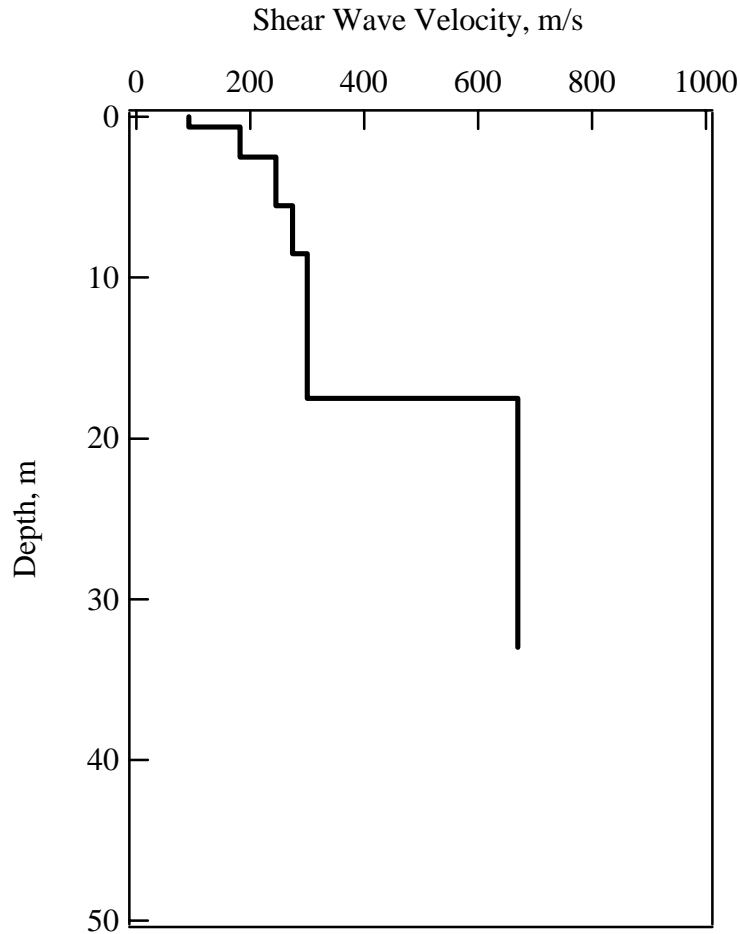


Figure 29 Shear Wave Velocity Profile Determined from SASW Testing at LD-12

**Ballica**

The Ballica (N 40.7799, E31.1019) station was a temporary aftershock station located in the free field. Ballica is a small town in the Duzce alluvial basin, south of the city of Duzce. Hammers and a bulldozer were used as wave sources and the SASW array was located approximately 75 m from the strong motion station.

The experimental and theoretical dispersion curves are shown in the appendix along with the tabulated  $V_S$  profile. The shear wave velocity profile from SASW testing is shown in Figure 8. Velocities below 200 m/s extend to a depth of 15 m and the measured velocity never exceeds 375 m/s. This profile is significantly softer than that measured at the Duzce strong motion station. This site is considered a soft soil site (Class E) in the Geomatrix classification system because of the 10 m of very soft material near the surface. The  $V_{S-30}$  for this site is 190 m/s, making it theoretically a stiff soil site ( $S_D$ ) in the UBC classification system. However, because the 10 m of material near the surface is most likely soft clay, the UBC classification is soft soil ( $S_E$ ).

### ***Aydinpinar***

The Aydinpinar (N 40.7526, E31.1132) station was a temporary aftershock station located in the free field. The station was situated at the base of the hills at the southern margin of the Duzce basin. Hammers and a drop weight were used as wave sources and the SASW array was located approximately 15 m from the strong motion station.

The experimental and theoretical dispersion curves are shown in the appendix along with the tabulated  $V_S$  profile. The shear wave velocity profiles from SASW testing are shown in Figure 30. Two shear wave velocity profile interpretations are shown in Figure 30, but both show similar trends. The shear wave velocity is around 300 m/s near the surface and reaches 450 m/s at a depth between 2.5 and 5 m. This 450 m/s layer extends at least to a depth of 20 m. Because the shear wave velocity profile does not extend beyond 20 m, it is difficult to classify this site. It is significantly stiffer than points in the interior of the Duzce basin (e.g. Duzce, Ballica stations), and probably can be classified as shallow soil (B) in the Geomatrix classification system. The  $V_{S-30}$  for this site is 430 m/s, based on extending the 450 m/s layer to 30 m. Therefore, this site is a soft rock/dense soil site ( $S_C$ ) in the UBC classification system.

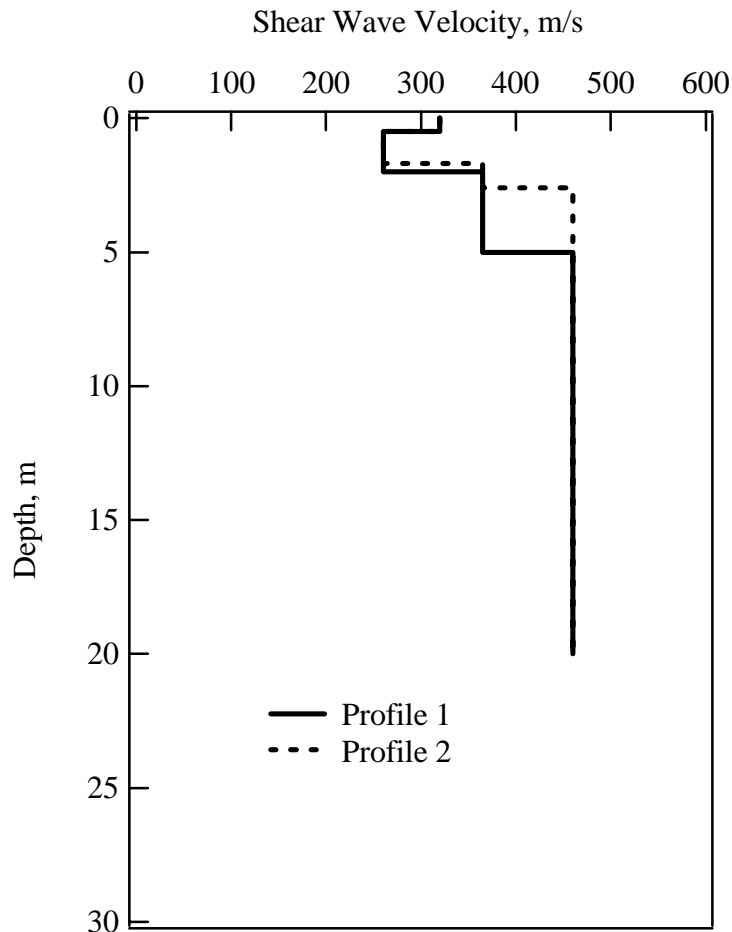


Figure 30 Shear Wave Velocity Profile Determined from SASW Testing at Aydinpinar (AYD)

***Hastane (Yalova)***

The Hastane (N 40.6526, E29.2632) station was a temporary aftershock station located in a reinforced concrete hospital building in the city of Yalova. The site is approximately 0.5 km from the shore of Izmit Bay and in an area of enhanced damage during the Izmit earthquake. Hammers and a drop weight were used as wave sources. We do not know the exact building on the hospital grounds where this station was housed, so we cannot estimate the distance between the SASW array and instrument location.

The experimental and theoretical dispersion curves are shown in the appendix along with the tabulated  $V_s$  profile. The shear wave velocity profile from SASW testing is shown in Figure 31. This profile extends only 10 m because of space and noise limitations in the area. The site is soft at the surface with velocities less than 150 m/s in the top 1.5 m. In the top 10 m, the shear wave velocity is less than 300 m/s, with most values less than 200 m/s. Because of the limited depth of profiling, it is not possible to classify this site.

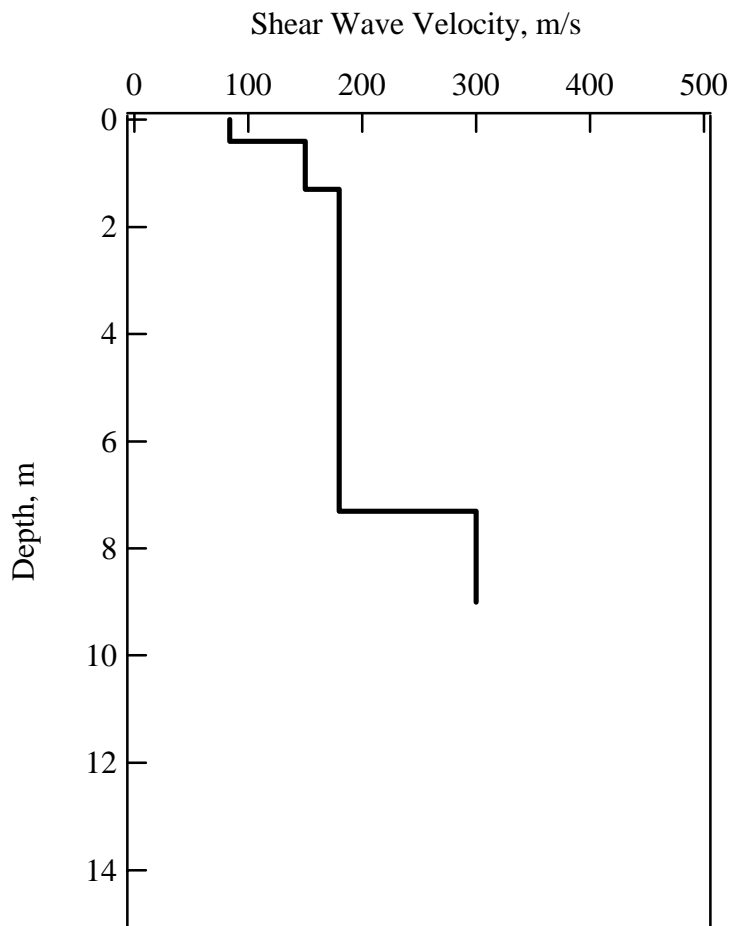


Figure 31 Shear Wave Velocity Profile Determined from SASW Testing at Hastane (HAS)

***Hilal (Yalova)***

The Hilal (N 40.6473, E29.2645) station was a temporary aftershock station located in the lowest level of a 3-story, reinforced concrete structure in the city of Yalova. The site is approximately 0.75 km south of the Hastane station in an area of moderate damage from the Izmit earthquake. This area is also uphill from the Hastane station. Hammers and a drop weight were used as wave sources and testing was performed on the roadway in front of the structure. The SASW array was located approximately 15 m from the strong motion station.

The experimental and theoretical dispersion curves are shown in the appendix along with the tabulated  $V_s$  profile. The shear wave velocity profile from SASW testing is shown in Figure 32. A very thin layer (0.5 m) of 300 m/s material is shown at the ground surface. This velocity is most likely due to the influence of the cobblestone roadway. Below the roadway, the material is significantly softer, with velocities below 150 m/s. This soft layer extends to at least 12 m. Because of the limited depth of profiling, it is not possible to classify this site. Interestingly, the Hilal profile is somewhat softer than Hastane, even though more damage was observed near Hastane. More research is needed to understand the damage patterns in Yalova.

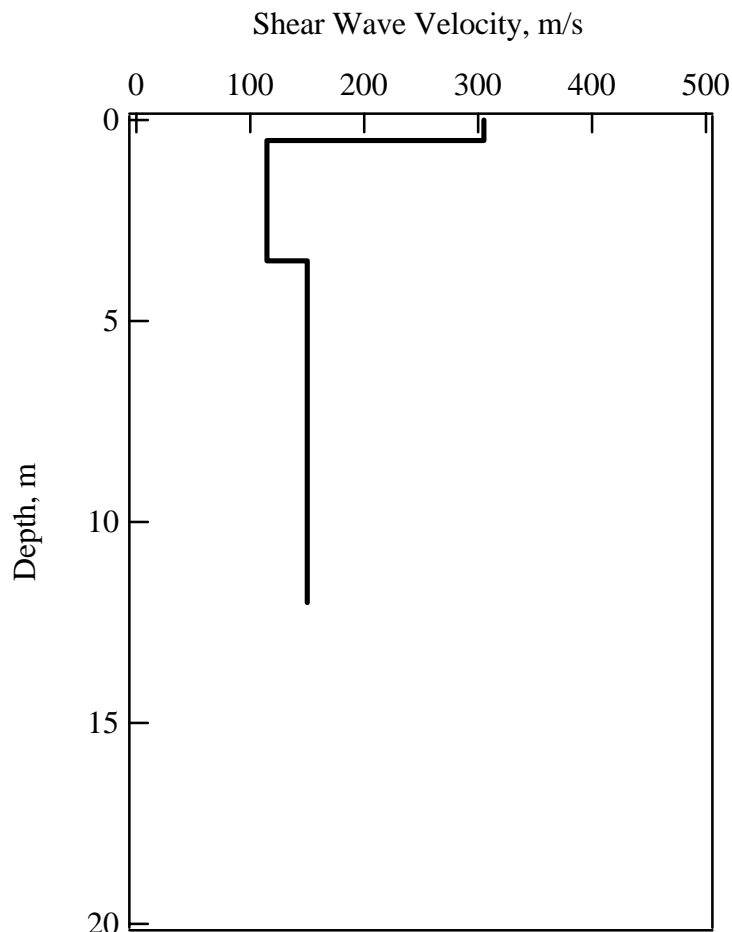


Figure 32 Shear Wave Velocity Profile Determined from SASW Testing at Hilal (HIL)

## Discussion of SASW and Microtremor Results

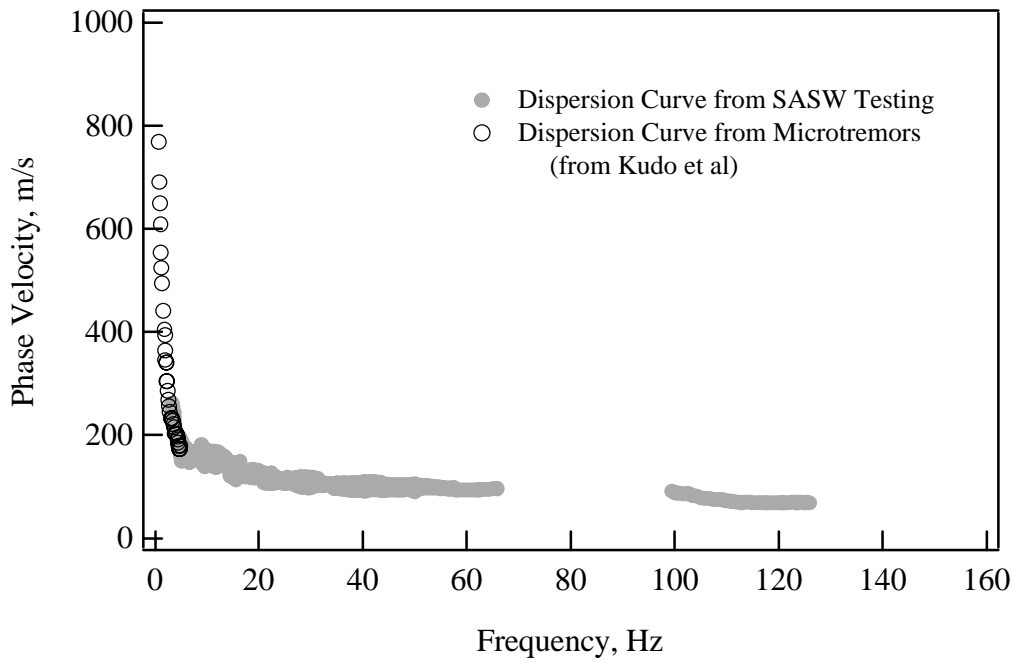
The testing performed in Turkey provides an interesting opportunity to compare two methods used to determine shear wave velocity profiles from surface wave motions. The 20 sites discussed in this report were characterized using the SASW method. The SASW method involves the use of active sources such as impact hammers, shakers, or random noise generators (i.e. bulldozers) to excite surface wave motions, as previously discussed in this report. At five of the sites characterized by the SASW method, shear wave velocity profiles were also determined from microtremors and aftershocks as discussed in detail in Kudo et. al., 2001. This method of surface wave analysis involves the use of low-frequency passive sources to determine the shear wave velocity profiles. The five sites that were tested with both methods are Ambarli (ATS), Cekmece (CNA), Duzce (DZC), Sakarya (SKR), and Yarimca (YPT). The comparison of shear wave velocity profiles determined from SASW testing and profiles determined from microtremors and aftershocks are shown in Figures 13, 16, 17, 23, and 24 for sites ATS, CNA, DZC, SKR, and YPT, respectively.

In comparing the profiles at each of these sites it was observed that the near-surface (~top 20 m) shear wave velocity values were often quite different between the two methods. It is useful to look at the measured dispersion curves from both methods to better understand the differences that were observed in the shear wave velocity profiles at these sites. Kudo et. al., 2001 presented dispersion curves from each of the five sites they evaluated. The authors of this report digitized these curves to obtain values to plot with the SASW results at these sites. The combined dispersion curves from sites ATS, CNA, DZC, SKR, and YPT are presented in Figures 33, 34, 35, 36, and 37, respectively. At three of the five sites, ATS, CNA, and YPT (Figures 33, 34 and 37, respectively) remarkable consistency is observed in the frequency range tested by both methods. This consistency is shown by the overlapping dispersion curves in the figures. At site DZC (Figure 35), the dispersion curves from the two methods appear to be discontinuous. This difference may be due to lateral variability that is observed due to the different scale of the two tests. At site SKR (Figure 36), common frequency ranges were not tested, and the variable SASW results made comparisons difficult.

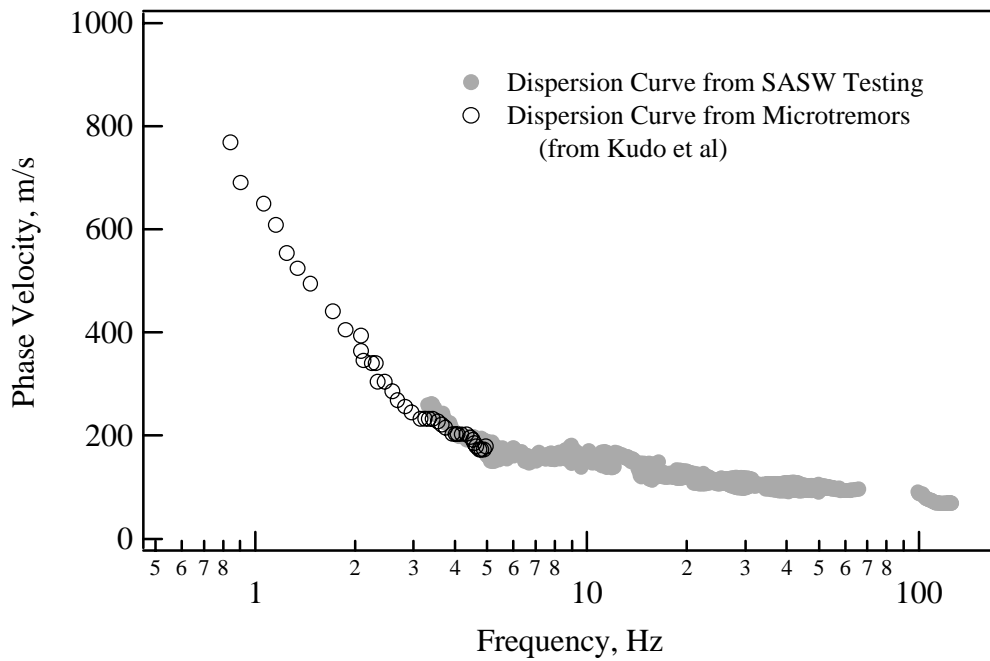
A second observation concerns the frequency content of the two tests. The microtremor results measure energy at very low frequencies and hence generate shear wave velocity profiles to great depth (1.5 km). On the other hand, the highest frequency measured by the microtremor method at these sites is on the order of 4 to 10 Hz. At these frequencies, the wavelengths measured at these sites is on the order of 40 to 100 m. In contrast, the SASW method measures frequencies in the range of 3-5 Hz on the low end to 150-300 Hz on the high end. The shortest wavelength measured with the SASW method at these sites is less than 1 m. Therefore, the SASW method is able to resolve the near-surface (top 40 m) shear wave velocity structure at these sites. The values reported from microtremor data really represent an extrapolation of the wave velocity into frequency ranges that were not measured. This can best be seen by comparing the measured dispersion curve from SASW testing with a theoretical dispersion curve generated from the profile determined with microtremor data. This comparison for site ATS is shown in Figure 38. The dispersion curve generated from the microtremor profile shows much higher surface wave velocities than were measured with SASW testing. The shear wave velocity profile determined from the microtremor measurements would result in overestimated  $V_{S-30}$

values and possible erroneous site classification. Therefore, although the microtremor method is a very useful means to determine deep shear wave velocity values, it generally should not be used for near-surface shear wave velocity evaluation and  $V_{S-30}$  calculations. In fact, it would be prudent if the  $V_S$  profile from the microtremor method was dashed in the upper depth region, say to a depth of 0.5 to 1.0 times the shortest wavelength resolved. This approach is used with the SASW method where the  $V_S$  profile is only presented to a depth of about one-half of the longest wavelength measured in the field.



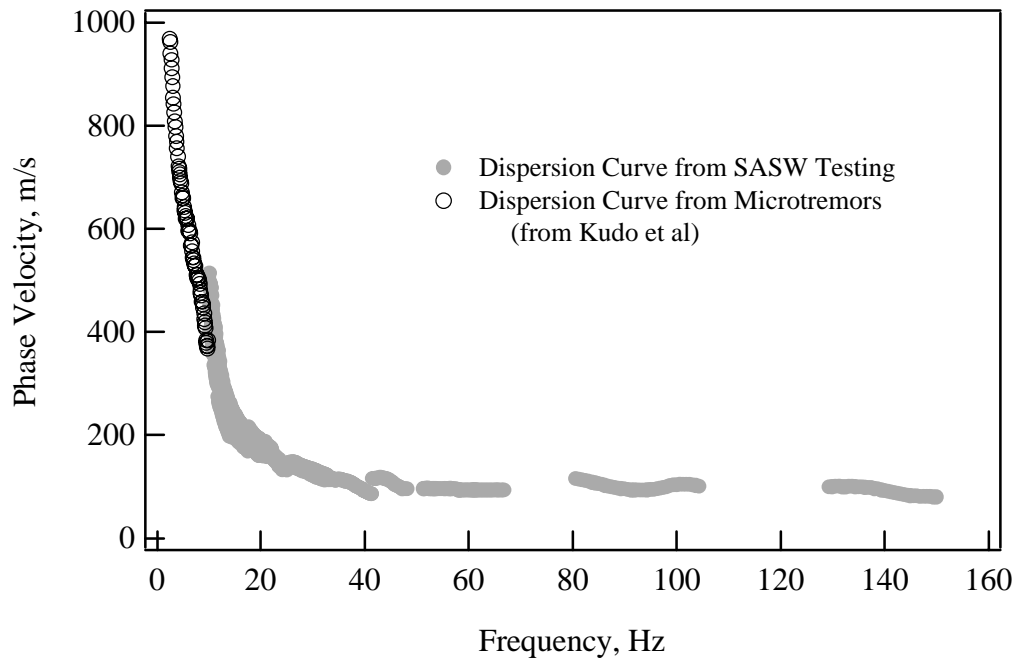


a. Experimental Dispersion Curves-Linear Frequency Scale

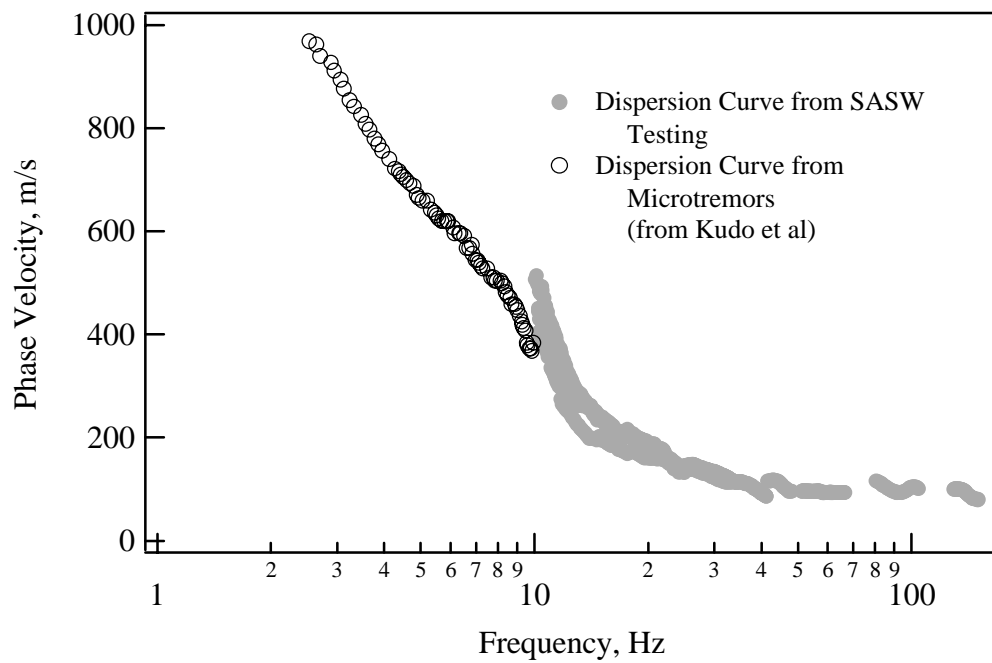


b. Experimental Dispersion Curves-Log Frequency Scale

Figure 33 Comparison of Dispersion Curves Measured with Active Sources (SASW) to Dispersion Curves Measured with Passive Sources (Kudo et al., 2001) at Ambarli (ATS)

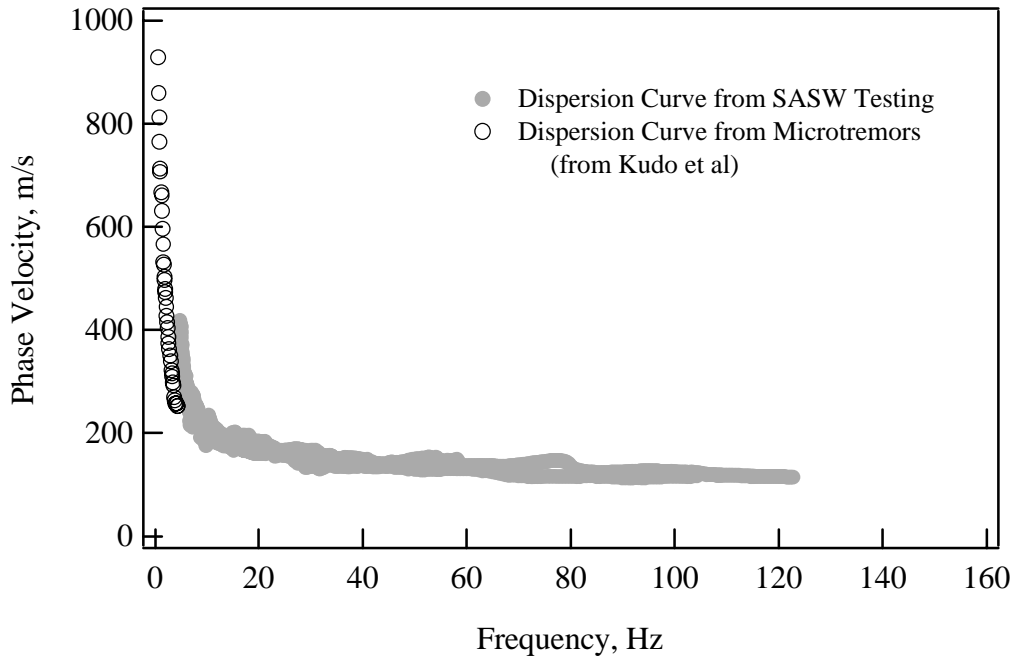


a. Experimental Dispersion Curves-Linear Frequency Scale

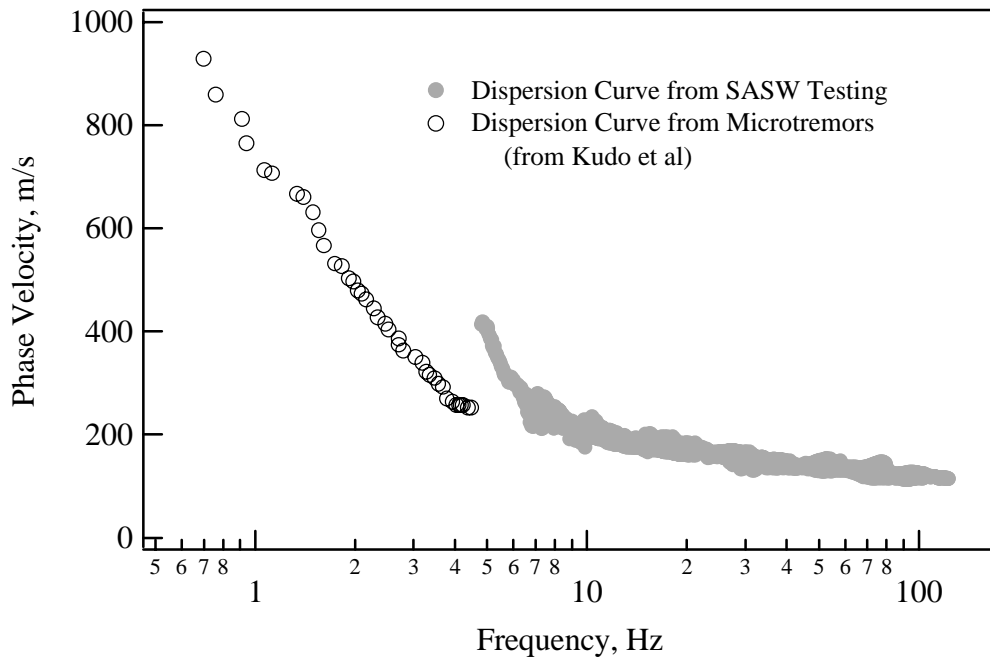


b. Experimental Dispersion Curves-Log Frequency Scale

Figure 34 Comparison of Dispersion Curves Measured with Active Sources (SASW) to Dispersion Curves Measured with Passive Source (Kudo et al., 2001) at Cekmece (CNA)

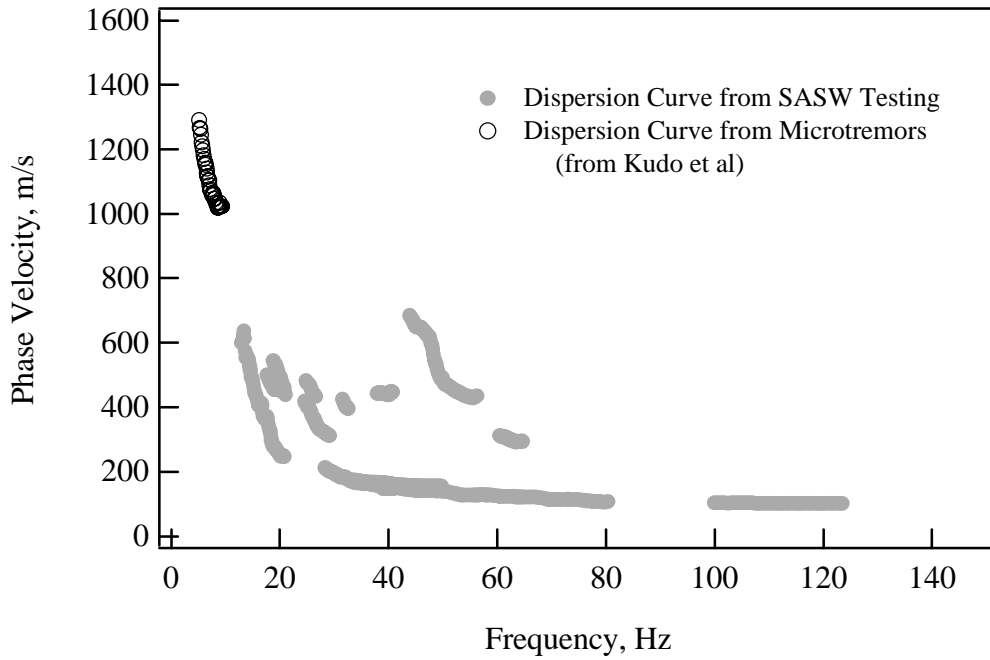


a. Experimental Dispersion Curves-Linear Frequency Scale

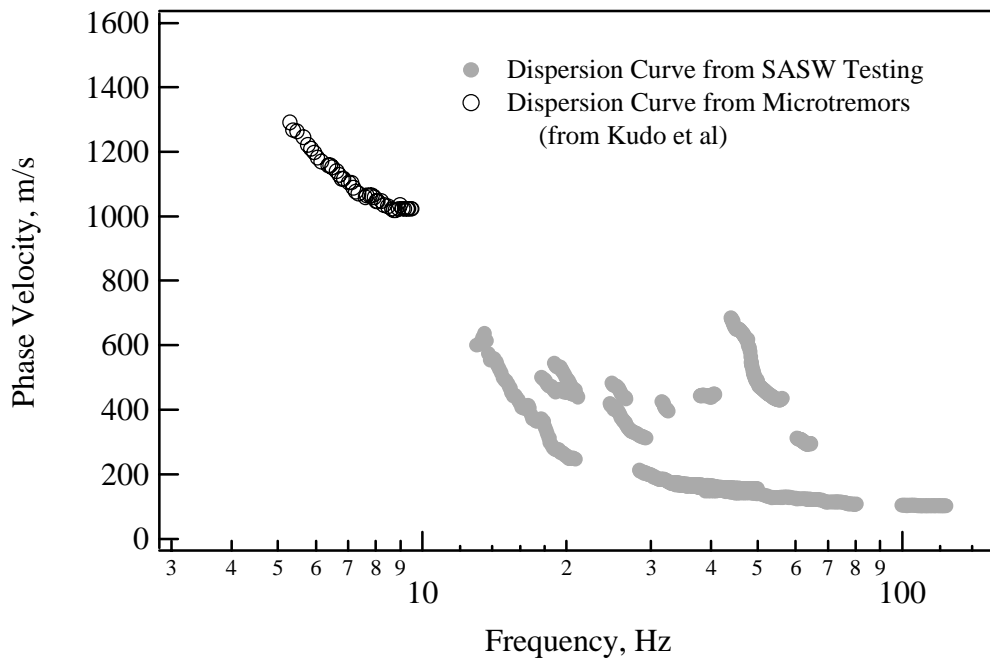


b. Experimental Dispersion Curves-Log Frequency Scale

Figure 35 Comparison of Dispersion Curves Measured with Active Sources (SASW) to Dispersion Curves Measured with Passive Source (Kudo et al., 2001) at Duzce (DZC)

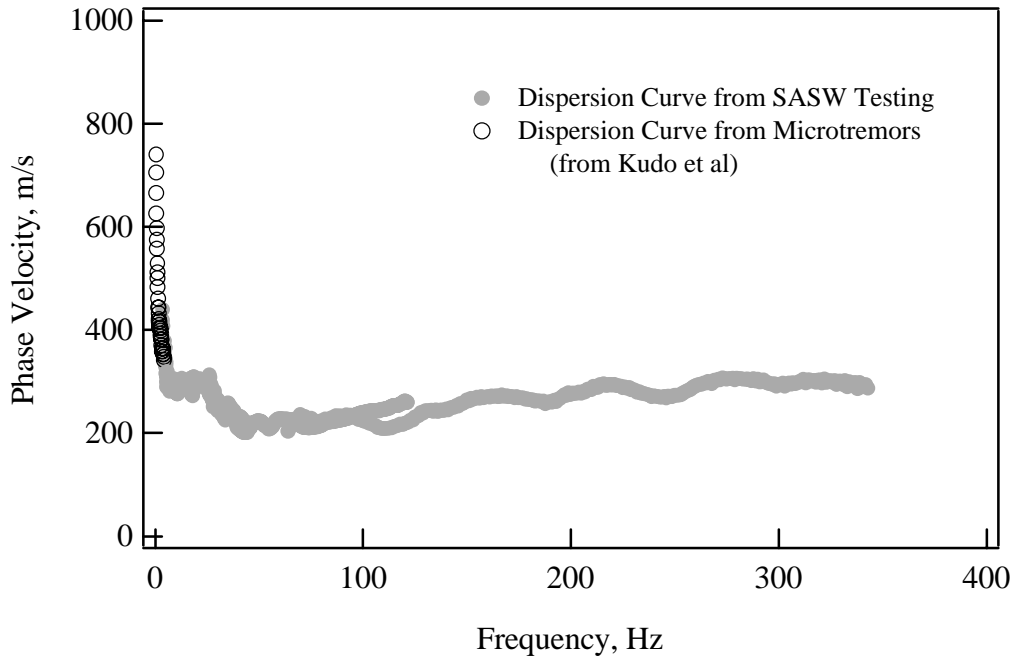


a. Experimental Dispersion Curves-Linear Frequency Scale

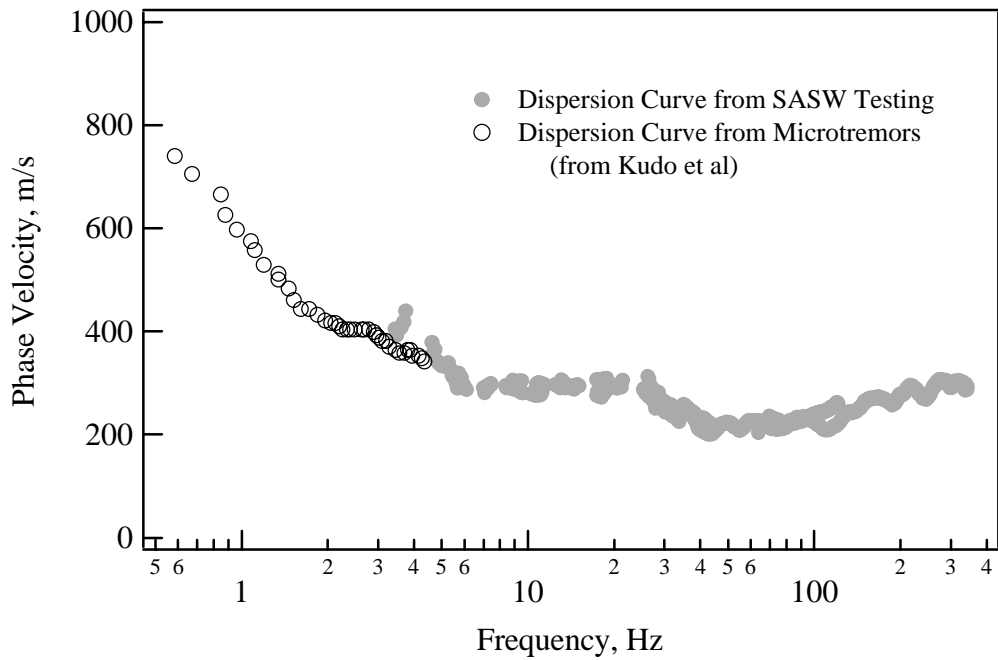


b. Experimental Dispersion Curves-Linear Frequency Scale

Figure 36 Comparison of Dispersion Curves Measured with Active Sources (SASW) to Dispersion Curves Measured with Passive Source (Kudo et al., 2001) at Sakarya (SKR)



a. Experimental Dispersion Curves-Linear Frequency Scale



b. Experimental Dispersion Curves-Log Frequency Scale

Figure 37 Comparison of Dispersion Curves Measured with Active Sources (SASW) to Dispersion Curves Measured from Passive Source (Kudo et. al., 2001) at Yarimca (YPT)

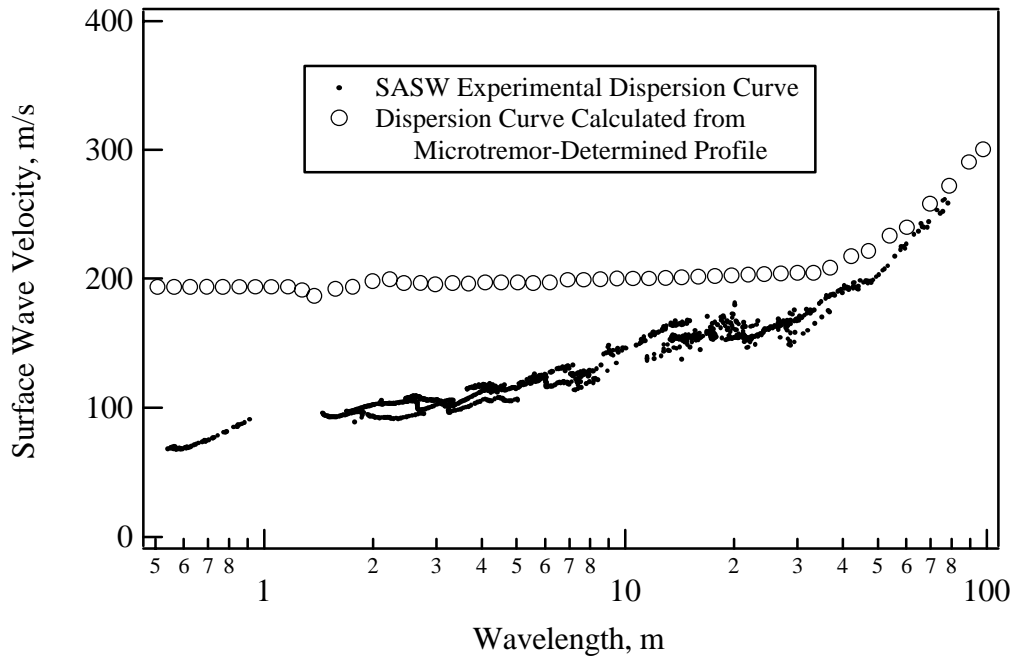


Figure 38 Comparison between the Measured Experimental Dispersion Curve from SASW Testing at ATS and the Theoretical Dispersion Curve Generated from the Shear Wave Velocity Profile Determined from Microtremor Measurements (Kudo et. al., 2001) at ATS

## Discussion of Site Classifications

The shear wave velocity profiles presented in this paper were used to classify the stations in terms of the Geomatrix (1993) and Uniform Building Code (ICBO 1997) site classification systems. The classifications for each station have been discussed previously and are listed in Table 5.

Often, strong motion stations are grouped into rock/shallow soil (Geomatrix Classes A/B) and deep soil (Geomatrix Classes C/D) when incorporated into attenuation relationships (e.g. Abrahamson and Silva 1997). Because of their unique response characteristics, soft soil sites (Class E) are not included in attenuation relationships. Silva (Personal communication 2001) has compiled shear wave velocity data collected at A/B and C/D sites in California. The 16<sup>th</sup>, 50<sup>th</sup>, and 84<sup>th</sup> percentile shear wave velocity profiles for A/B and C/D sites in California are shown in Figures 39 and 40, respectively. Additionally, the measured shear wave velocity profiles from Turkey for each site class are indicated.

In general, the Turkey data for A/B sites are bound by the 16<sup>th</sup> and 84<sup>th</sup> percentile curves from California (Fig. 43). The two curves that fall significantly above the 84<sup>th</sup> percentile curves are from Gebze and Izmit, two of only three true rock sites (Class A) tested as part of this study. These sites should have shear wave velocities that are above the median values for site classes A and B grouped together.

For the C/D sites (Figure 40), the Turkey data is again generally bound by the 16<sup>th</sup> and 84<sup>th</sup> percentile curves from California. However, most of the data fall at or above the median curve, and the Iznik, Yarimca, and Cekmece stations show velocities above the 84<sup>th</sup> percentile curve. At Iznik and Yarimca, only thin layers of high velocity material are present, but high velocity layers extend to a depth of 20 m at Cekmece. The higher average velocities at Turkey C/D sites may result from the limited number of C/D sites tested as part of this study.

The shear wave velocity profiles from soft soil sites (Class E) at Ambarli and Ballica are shown in Figure 41, along with the 16<sup>th</sup> and 84<sup>th</sup> percentile curves for C/D sites in California. At depths less than 25 m, the Ambarli profile falls significantly below the 16<sup>th</sup> percentile curve and Ballica falls at the 16<sup>th</sup> percentile curve. The very low velocities at Ambarli certainly contributed to the large ground motions recorded there, 79 km away from the fault rupture of the Izmit earthquake. Ballica is an aftershock station and did not record the main shocks of the Kocaeli and Duzce earthquakes.

Table 5 Site Classification of Strong Motion Stations Tested as Part of this Study.

| Station (Owner <sup>1</sup> ) | Geomatrix Site Class | V <sub>s-30</sub> (m/s) | UBC Site Class                 |
|-------------------------------|----------------------|-------------------------|--------------------------------|
| Arcelik – ARC (K)             | B                    | 360-500                 | S <sub>C</sub>                 |
| Ambarli – ATS (K)             | E                    | 175                     | S <sub>E</sub>                 |
| Bolu – BOL (E)                | D                    | 290                     | S <sub>D</sub>                 |
| Cekmece – CNA (K)             | D                    | 350                     | S <sub>D</sub>                 |
| Duzce – DZC (E)               | D                    | 275                     | S <sub>D</sub>                 |
| Gebze – GBZ (E)               | A                    | 750                     | S <sub>B</sub>                 |
| Izmit – IZN (E)               | D                    | 180-190 <sup>1</sup>    | S <sub>E</sub> /S <sub>D</sub> |
| Izmit – IZT (E)               | A                    | 800 <sup>1</sup>        | S <sub>B</sub>                 |
| Sakarya – SKR (E)             | B                    | 470 <sup>1</sup>        | S <sub>C</sub>                 |
| Yarimca – YPT (K)             | D                    | 300                     | S <sub>D</sub>                 |
| LD-3 (L)                      | B                    | 520 <sup>1</sup>        | S <sub>C</sub>                 |
| LD-5 (L)                      | A                    | 660 <sup>1</sup>        | S <sub>C</sub>                 |
| LD-7 (L)                      | B                    | - <sup>2</sup>          | -                              |
| LD-9 (L)                      | B                    | 500-800 <sup>1</sup>    | S <sub>C</sub> /S <sub>B</sub> |
| LD-10 (L)                     | B                    | 480                     | S <sub>C</sub>                 |
| LD-12 (L)                     | B                    | 340                     | S <sub>D</sub>                 |
| Ballica – BAL (K)             | E                    | 190                     | S <sub>E</sub>                 |
| Aydinpinar – AYD (K)          | B                    | 430 <sup>1</sup>        | S <sub>C</sub>                 |
| Hastane – HAS (K)             | - <sup>2</sup>       | - <sup>2</sup>          | -                              |
| Hilal – HIL (K)               | - <sup>2</sup>       | - <sup>2</sup>          | -                              |

<sup>1</sup> SASW profiling extended less than 30 m. Extrapolated to obtain V<sub>s-30</sub>.

<sup>2</sup> SASW profiling extended less than 10 m and was not extrapolated to 30 m.



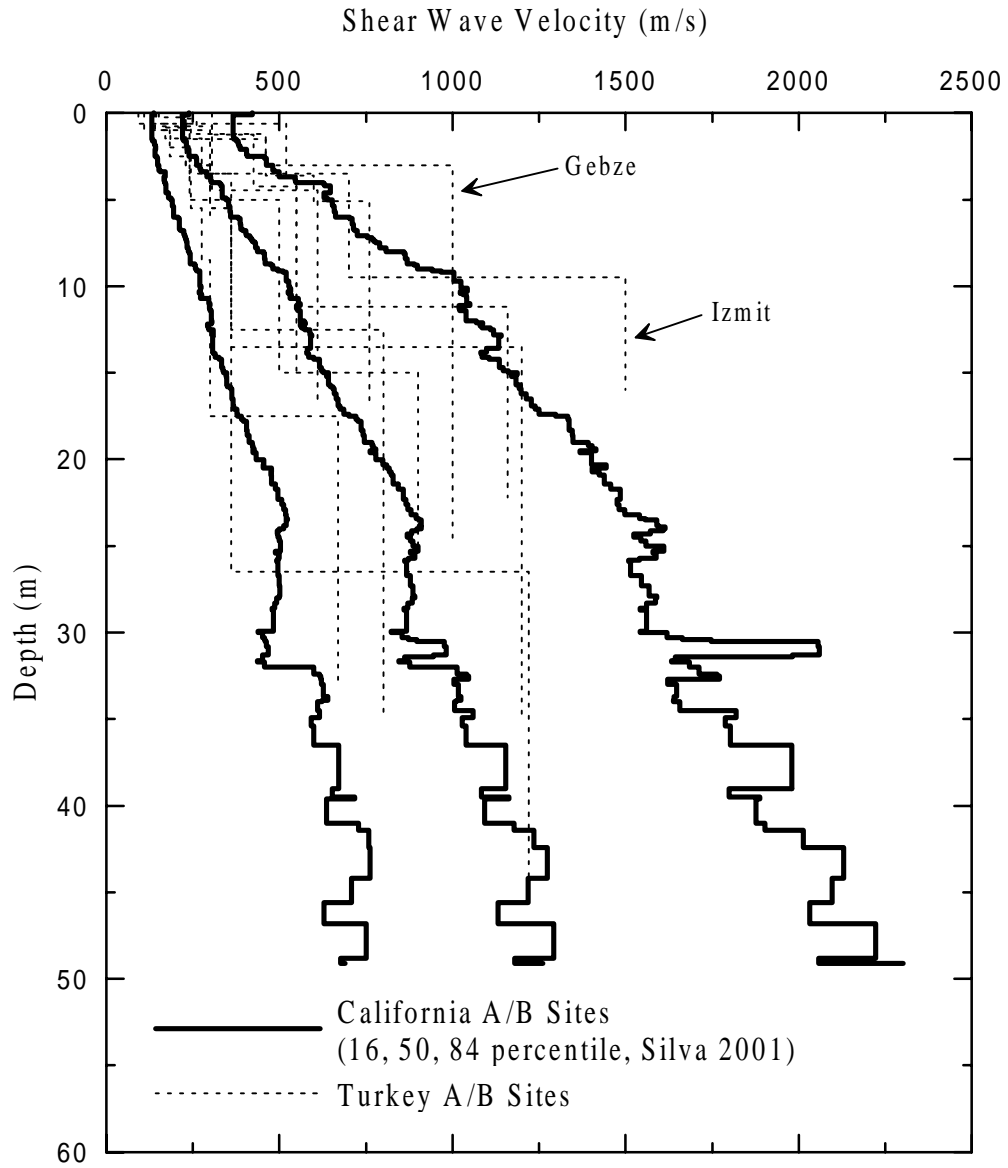


Figure 39 16<sup>th</sup>, 50<sup>th</sup>, And 84<sup>th</sup> Percentile Shear Wave Profiles For A/B Sites in California (Silva 2001) and Measured Shear Wave Profiles for A/B Sites in Turkey

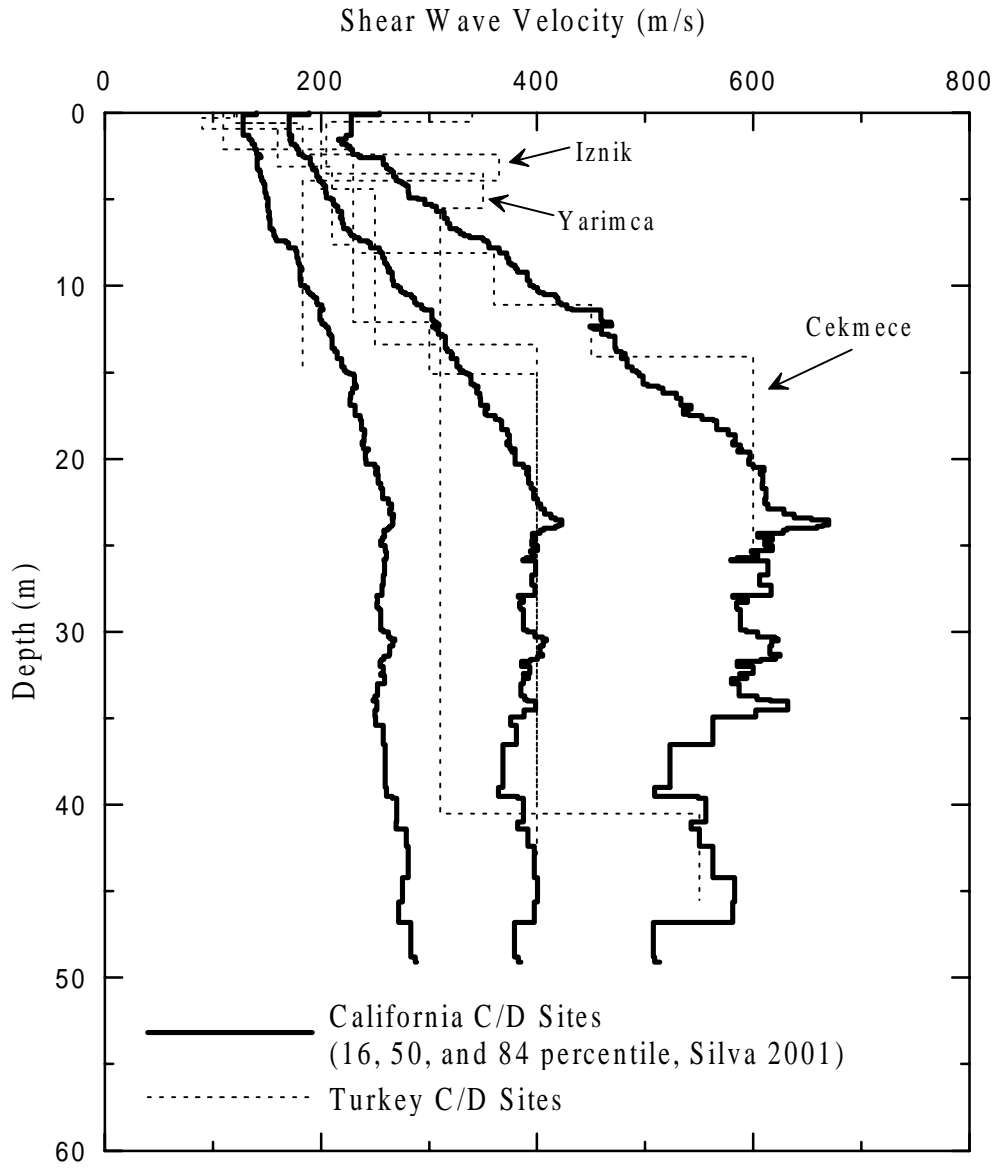


Figure 40 16<sup>th</sup>, 50<sup>th</sup>, And 84<sup>th</sup> Percentile Shear Wave Profiles for C/D Sites in California (Silva 2001) and Measured Shear Wave Profiles from C/D Sites in Turkey

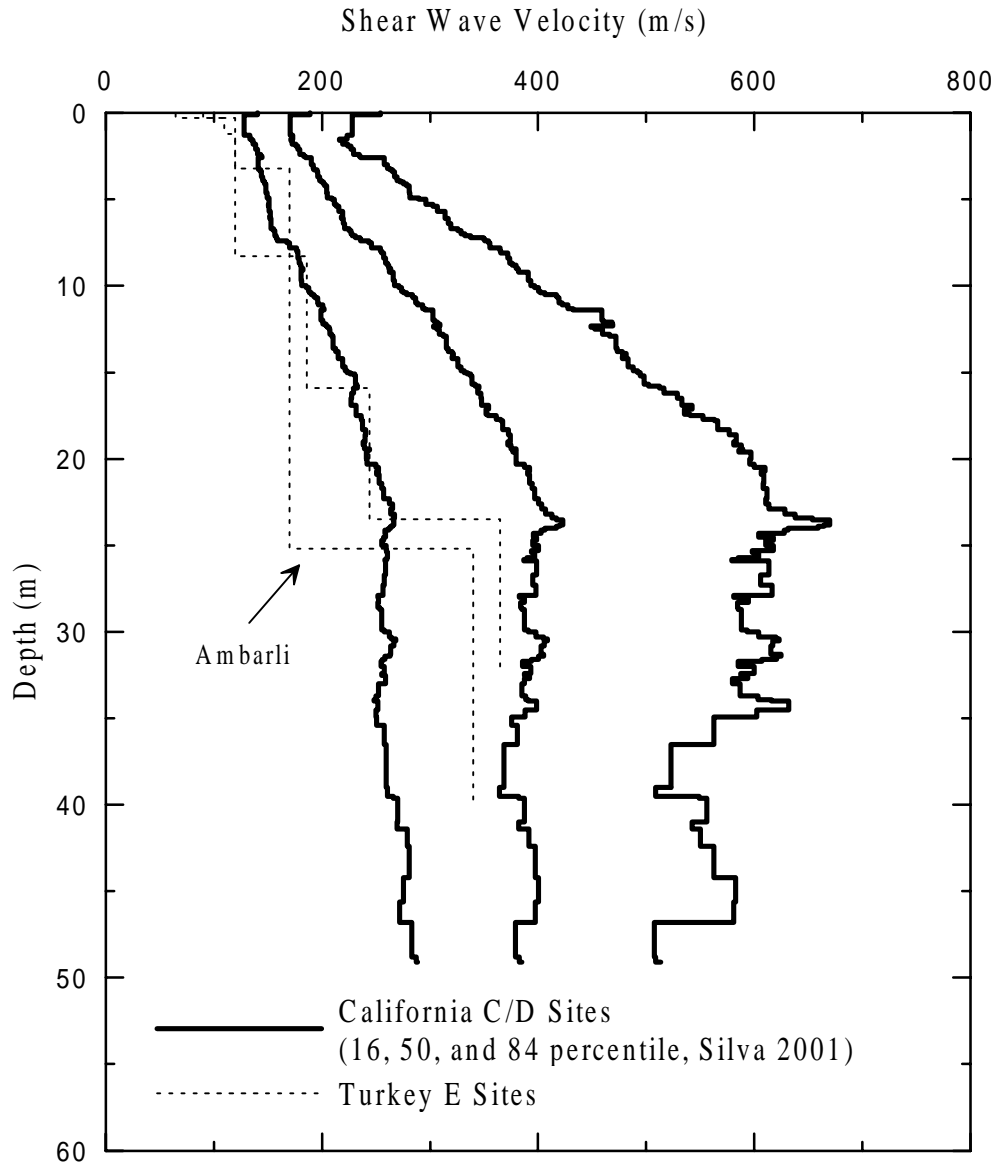


Figure 41 16<sup>th</sup>, 50<sup>th</sup>, and 84<sup>th</sup> Percentile Shear Wave Profiles for C/D Sites in California (Silva 2001) and Measured Shear Wave Profiles from E Sites in Turkey

## **Future Research Collaborations**

This project was successful in characterizing the shear wave velocity profiles at 16 strong motion stations and 4 aftershock stations in Turkey. Additionally, the field testing took less than two weeks to finish. Our significant research collaborators were Prof. Mustafa Erdik of the Kandilli Observatory and Earthquake Research Institute and geophysicist Dr. Ugur Kuran. Through this project these Turkish researchers became familiar with the SASW field testing technique. There are many possible projects in Turkey that could benefit from further SASW field testing.

Strong-Motion Station Characterization. This project focused mainly on the near-fault recording stations that recorded the Izmit and Duzce earthquakes. However, there are more than ten other stations that recorded these earthquakes where shear wave velocities have not been measured. Many of these stations are located in Istanbul, where ground motion characterization for a future large earthquake on the North Anatolian fault is a major concern.

Geologic maps indicate that western Istanbul is founded mainly on consolidated, Tertiary sediments. However, some preliminary shear wave velocities measured by Ansal (Personal communication 2001) indicate that soil depths in this area are over 100 m. The discrepancy between the geologic maps and preliminary shear wave velocity profiles could be studied through SASW measurements (or any other  $V_s$  measurement technique) at the strong-motion stations in this area.

Damage Patterns. This project measured shear wave velocities at two sites within Yalova, in an attempt to correlate shear wave velocity with damage patterns. However, because of noise, wave source, and space limitations, the velocity profiles did not extend to a significant depth and could not be correlated with damage. In the future, better planning and wave sources could be used to profile deeper. Therefore, SASW testing could be used to measure shear wave velocities throughout the city of Yalova in an effort to understand damage patterns. The same procedure could be used to study damage patterns in Avcilar in western Istanbul.

Basin Modeling. Large, alluvial basins (e.g. Sakarya, Duzce basins) were shaken during the Izmit and Duzce earthquakes. Only one recording was made in each of these basins during the main events, but temporary stations were placed throughout these basins and recorded many aftershocks. These aftershock stations can help seismologists and engineers understand basin response and calibrate basin response programs. However, the shear wave velocity structure throughout the basin is needed to model the basin response accurately. SASW testing could be used to evaluate the shear wave velocity structure throughout alluvial basins in Turkey.

## **Acknowledgements**

The authors gratefully acknowledge the financial support provided by the National Science Foundation under grant CMS-0085300 and the Pacific Earthquake Engineering Research Center Lifelines Program. Additionally, the assistance of Prof. Mustafa Erdik and Mr. Cem Ozbey of the Kandilli Observatory and Earthquake Research Institute, and geophysicists Dr. Ugur Kuran and Mr. Halit Kaya while in Turkey is greatly appreciated.

## References

- Abrahmson, N.A. and Silva, W.J. (1997) "Empirical Response Spectral Attenuation Relations for Shallow Crustal Earthquakes," *Seismological Research Letters*. 68(1) pp.94-127.
- Ansal, A. (2001) Personal communication.
- EERI (2000) *The Izmit (Turkey) Earthquake of August 17, 1999: A Reconnaissance Report*, Earthquake Engineering Research Institute.
- Geomatrix Consultants (1993) "Compilation of Geotechnical Data for Strong-Motion Stations in the Western United States," Report to Lawrence Livermore National Laboratory, Project No. 2256.
- Gucunski, N. and Woods, R.D., (1991), "Instrumentation for SASW Testing," *Geotechnical Special Publication No. 29 Recent Advances in Instrumentation, Data Acquisition and Testing In Soil Dynamics*, American Society of Civil Engineers, 1-16 pp.
- International Council of Building Officials (1997) *Uniform Building Code*, Whittier, CA.
- Joh, S.-H. (1996) "Advances in Interpretation and Analysis Techniques for Spectral-Analysis-of-Surface-Waves(SASW) Measurements", Ph.D. Dissertation, University of Texas at Austin, Austin, TX.
- Kausel, E. and Roesset, J.M. (1981), "Stiffness Matrices for Layered Soils," *Bulletin of the Seismological Society of America*, Vol. 71, No. 6, December, pp. 1743-1761.
- Kudo, K., Kanno, T., Okada, H., Ozel, O., Erdik, M., Takahashi, M., Sasatani, T., Higashi, S., Yoshida, K. (2001), "Site Specific Issues on Strong Ground Motion during the Kocaeli, Turkey Earthquake of August 17, 1999, as Inferred from Array Observations of Microtremors and Aftershocks," Submitted to Bulletin of the Seismological Society of America, August 10, 2000.
- Rix, G., and Stokoe, K.H., II (1989), "Stiffness Profiling of Pavement Subgrades," *Transportation Research Record No. 1235*, pp. 1-9.
- Silva (2001) Personal communication.
- Stokoe, K.H., Wright, S.G., Bay, J.A., and Roesset, J.M., (1994), "Characterization of Geotechnical Sites by SASW Method," *Technical Review: Geophysical Characterization of Sites*, ISSMFE Technical Committee 10, edited by R.D. woods, Oxford Publishers, New Delhi.
- Stokoe, K.H., M.B Darendeli, R.D. Andrus and L.T. Brown (1999) "Dynamic Soil Properties: Laboratory, Field and Correlation Studies," Theme Lecture, *Second International Conference Earthquake Geotechnical Engineering*, Vol. 3, Lisbon, Portugal, June, pp. 811-845.